BRIGHAM YOUNG UNIVERSITY

GEOLOGY STUDIES

GEOLOGICAL SOCIETY OF AMERICA

FIELD TRIP GUIDE BOOK

1997 ANNUAL MEETING • SALT LAKE CITY, UTAH

PART 2 TWO

EDITED BY PAUL KARL LINK AND BART J. KOWALLIS

VOLUME 42 • 1997

MESOZOIC TO RECENT GEOLOGY OF UTAH

Edited by
Paul Karl Link and Bart J. Kowallis

BRIGHAM YOUNG UNIVERSITY GEOLOGY STUDIES

Volume 42, Part II, 1997

CONTENTS

A Publication of the
Department of Geology
Brigham Young University
Provo, Utah 84602

Brigham Young University Geology Studies is published by the Department of Geology. This publication consists of graduate student and faculty research within the department as well as papers submitted by outside contributors. Each article submitted is externally reviewed by at least two qualified persons.

Cover photos taken by Paul Karl Link.

Top: Upheaval Dome, southeastern Utah.
Middle: Lake Bonneville shorelines west of Brigham City, Utah.
Bottom: Bryce Canyon National Park, Utah.

ISSN 0068-1016
9-97 700 23870/24290

Preface

Guidebooks have been part of the exploration of the American West since Oregon Trail days. Geologic guidebooks with maps and photographs are an especially graphic tool for school teachers, University classes, and visiting geologists to become familiar with the territory, the geologic issues and the available references.

It was in this spirit that we set out to compile this two-volume set of field trip descriptions for the Annual Meeting of the Geological Society of America in Salt Lake City in October 1997. We were seeking to produce a quality product, with fully peer-reviewed papers, and user-friendly field trip logs. We found we were bucking a tide in our profession which de-emphasizes guidebooks and paper products. If this tide continues we wish to be on record as producing "The Last Best Geologic Guidebook."

We thank all the authors who met our strict deadlines and contributed this outstanding set of papers. We hope this work will stand for years to come as a lasting introduction to the complex geology of the Colorado Plateau, Basin and Range, Wasatch Front, and Snake River Plain in the vicinity of Salt Lake City. Index maps to the field trips contained in each volume are on the back covers.

Part 1 "Proterozoic to Recent Stratigraphy, Tectonics and Volcanology: Utah, Nevada, Southern Idaho and Central Mexico" contains a number of papers of exceptional interest for their geologic synthesis. Part 2 "Mesozoic to Recent Geology of Utah" concentrates on the Colorado Plateau and the Wasatch Front.

Paul Link read all the papers and coordinated the review process. Bart Kowallis copy edited the manuscripts and coordinated the publication via Brigham Young University Geology Studies. We would like to thank all the reviewers, who were generally prompt and helpful in meeting our tight schedule. These included: Lee Allison, Genevieve Atwood, Gary Axen, Jim Beget, Myron Best, David Bice, Phyllis Camilleri, Marjorie Chan, Nick Christie-Blick, Gary Christenson, Dan Chure, Mary Droser, Ernie Duebendorfer, Tony Ekdale, Todd Ehlers, Ben Everitt, Geoff Freethey, Hugh Hurlow, Jim Garrison, Denny Geist, Jeff Geslin, Ron Greeley, Gus Gustason, Bill Hackett, Kimm Harty, Grant Heiken, Lehi Hintze, Peter Huntoon, Peter Isaacson, Jeff Keaton, Keith Ketner, Guy King, Mel Kuntz, Tim Lawton, Spencer Lucas, Lon McCarley, Meghan Miller, Gautam Mitra, Kathy Nichols, Robert Q. Oaks, Susan Olig, Jack Oviatt, Bill Perry, Andy Pulham, Dick Robison, Rube Ross, Rich Schweickert, Peter Sheehan, Norm Silberling, Dick Smith, Barry Solomon, K.O. Stanley, Kevin Stewart, Wanda Taylor, Glenn Thackray and Adolph Yonkee. In addition, we wish to thank all the dedicated workers at Brigham Young University Print Services and in the Department of Geology who contributed many long hours of work to these volumes.

Paul Karl Link and Bart J. Kowallis, Editors

Sequence Architecture and Stacking Patterns in the Cretaceous Foreland Basin, Utah: Tectonism versus Eustasy

P. SCHWANS
Exxon Exploration Company, P.O. Box 4778, Houston, Texas 77060-4778

K.M. CAMPION
Exxon Production Research Company, P.O. Box 2189, Houston, Texas 99252-2189

ABSTRACT

The field trip examines the variations in depositional architecture, stacking patterns, and unconformity expression in strata deposited at the Cretaceous foreland basin margin in central Utah. Two sediment accommodation zones are identified. A zone proximal to the thrust front (<150 km distance) with high basin subsidence and sediment accommodation features predominantly alluvial deposits and sequences bounded by merged 3rd-order and angular unconformities; airy-isostatic subsidence dominated here. In a second zone located farther basinward (>150 km distance) basin subsidence and sediment accommodation decrease to the east and the basin fill is predominantly transitional alluvial to shallow-marine. Sequences are bounded by higher frequency unconformities and their correlative conformities; flexural subsidence dominates here and defines a ramp. Sequence expression and stacking patterns are explained within an accommodation cycle of basin subsidence and sea level change. This can be are used to better understand the influence of structuring versus eustasy on depositional architecture.

INTRODUCTION

Sequence stratigraphy concepts were originally developed from shallow-marine successions along passive margins where subsidence increases basinward, shelf edges separate shallow-water from deep-water environments, and tectonic events are muted (Vail et al., 1977, 1984; Haq et al., 1987, 1988, Jervey, 1988; Posamentier and Vail, 1988; Posamentier et al., 1988). Over the last several years sequence-stratigraphy has been increasingly applied and tested in foreland basins, where basin subsidence increases toward an active fold belt, strata are deposited across a ramp of uniform dip, and deep-water environments are absent. Consequently, the applicability of sequence stratigraphy concepts in foreland basins and the impact of tectonism on stratal patterns have been scrutinized; examples, among others, are the work by Weimer (1984), Jervey (1988), Jordan and Flemings (1991), Schwans (1990, 1991, 1995), Walker and Eyles (1991), Posamentier et al., (1992), Devlin et al., (1993), Gardner (1993), Martinsen, et. al., (1993), and Leithold (1994).

PREVIOUS WORK

Previous stratigraphic work on the transitional alluvial to shallow-marine foreland basin strata in central Utah, commonly referred to as Indianola Group, utilized formational attributes and sparse biostratigraphic strata. Pioneering studies are those of Spieker and Reeside (1925) and Spieker (1946, 1949). More recent examples are the works of Hale and Van De Graff (1964), Gill and Hail (1975), Cobban (1976), Lawton (1982, 1983, 1985), Ryer (1981), Ryer and McPhillips (1983), Fouch et al., (1983), and more recently Franczyk et al., (1992), among others. A different approach was taken by Schwans (1988a, 1988b, 1995), who placed facies and similarities in stratal successions and stacking patterns into a biostratigraphic and sequence-stratigraphic framework; Figure 1 shows the resulting chronostratigraphy. The hiatus of the unconformities and the age of sequences in the chart are based on biostratigraphic and absolute age data discussed in detail in Schwans (1985a, 1986a, 1988a, 1988b, 1995); discussed are also the relationship between the sequence framework (Fig. 1) and the existing formation

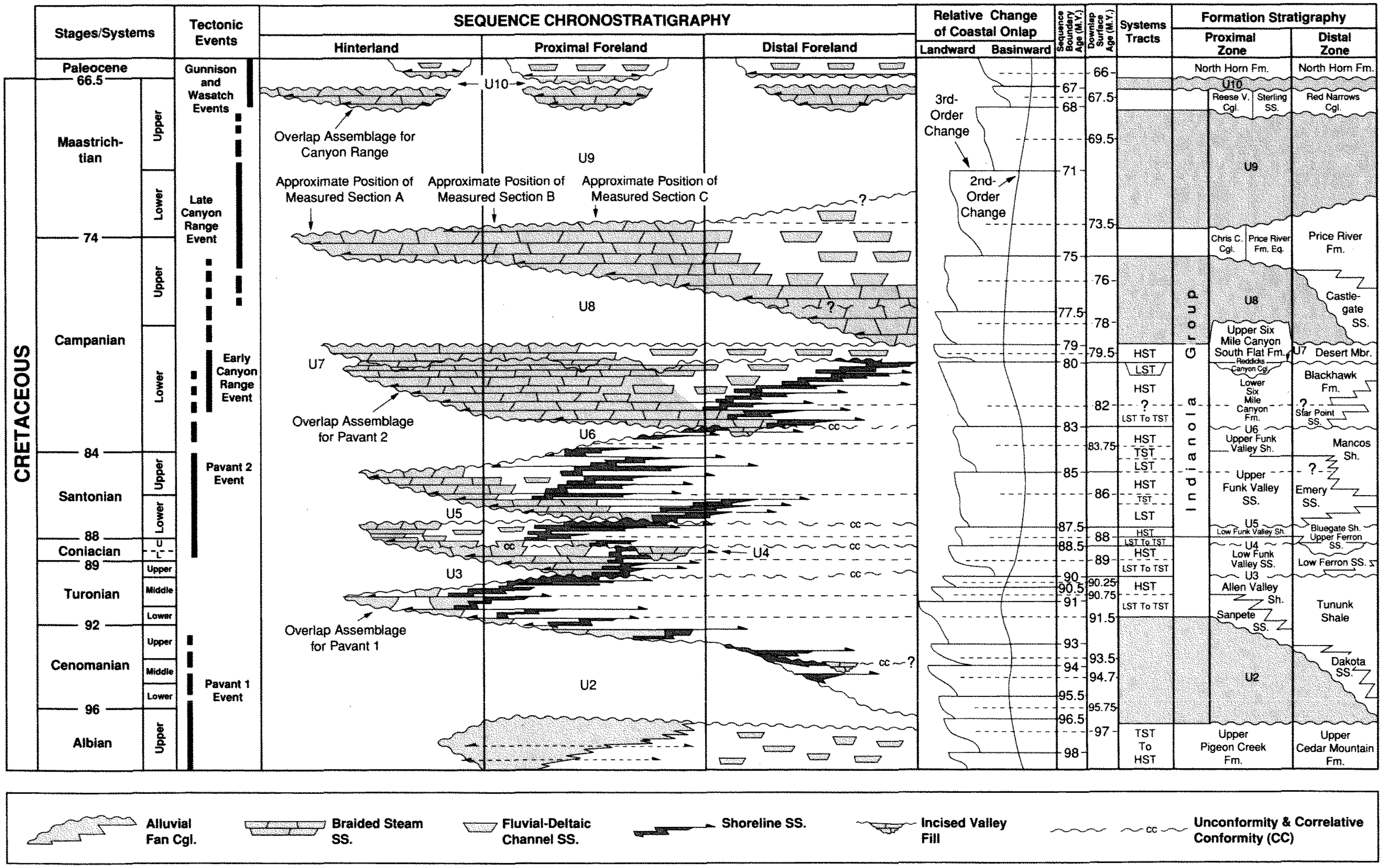

Figure 1. Sequence chronostratigraphy of the Cretaceous foreland basin in Utah with formations and interpreted tectonic events indicated. Ages of formations and timing of tectonic events are based on biostratigraphic and other age data discussed in Schwans (1988a, 1988b, 1995). The curves of relative change of coastal onlap are after Haq et al., (1987, 1988). LST–Lowstand systems tract; HST–Highstand systems tract; TST–Transgressive systems tract.

stratigraphy. The curve of coastal onlap and the ages of sequence boundaries and downlap surfaces from Haq et al., (1987) are included to provide comparison between the cyclicities observed in the foreland basin and at passive margin worldwide. Other studies on Cretaceous sequence stratigraphy in the foreland basin include, among others, Schwans (1986b, 1989, 1995), Vail and Bowman (1987), Aubrey (1989), Shanley and McCabe (1991, 1995), Van Wagoner (1991a, 1991b, 1995), and Van Wagoner et al., (1990). Figure 2 is a location map of the field trip area with the stops indicated.

STRUCTURE AND FORELAND BASIN ZONATION

Structure

The field trip area straddles a major structural transition zone the *Cordilleran hingeline.* Picha (1986) describes the *hingeline* as a zone that separates thick cratonic crust to the east from thinned, late Proterozoic-rifted crust in the west. Paleozoic miogeoclinal strata above basement thicken westward of the *hingeline* from 1000 m beneath the Wasatch Plateau to 11,000 m at the Utah-Nevada border (Standlee, 1982). The western portion of the Cretaceous foreland basin lies within this *hinge zone* (Schwans, 1988a, 1988b, 1995). Figure 3 shows the structural elements that influenced the configuration of the foreland basin in Utah; these are: (1) Proterozoic-rifted basement structures, (2) basement lineaments, and (3) Cretaceous-Tertiary thrust-fold structures.

Basement highs defined the position of the Mesozoic thrust ramps and the Cenozoic thrust-cored anticlines (Allmendinger et al., 1986, 1987; Lawton et al., 1994; Schwans, 1987a, 1987b, 1995). Intervening basement lows influenced the geographic configuration and position of alluvial to lacustrine Cenozoic basins. The eastern margin of the *hinge zone* is defined by the *Ephraim Fault* (EF in Fig. 3); basement is downthrown to the west to 9 km depth (Allmendinger et al., 1987).

Three basement lineaments or transverse faults cross the field trip area. The lineaments originated during Proterozoic rifting and were reactivated during Cretaceous-Tertiary compression as tear faults or right-lateral ramps to the eastward propagating thrusts (Fig. 3). In addition, the lineament acted as sediments conduits, linking the alluvial basins in the thrust belt to the marine foreland basin. Figure 4 is an interpreted seismic line across the field trip area; the interpretation is tied to measured section B (Stops 3.3, 3.4 in Fig. 2) and C (Stops 2.4, 2.5, 2.6 in Fig. 2) and two wells. Together, the figures illustrate the configuration of the thrust systems. The Pavant 1 (P1), Pavant 2 (P2), and the Canyon Range (C) thrust are Mesozoic thrusts, while the Gunnison (G) and Wasatch (W) thrusts are of early Cenozoic age; the latter terminate as blind thrusts in Jurassic strata underneath the Wasatch Plateau (Standlee, 1982; Lawton, 1985; Villien and Kligfield, 1986). Figure 5 shows the interpreted structural and stratigraphic history of the fold-thrust belt in central Utah by Schwans (1988b, 1995). Alternate views and an expanded discussions are by Lawton and Trexler (1991), Royse (1993), Lawton et al., (1994), DeCelles et al., (1995), and Talling et al., (1995).

Zonation

Schwans (1995) discussed in detail the structural and stratigraphic zonation of the Cretaceous foreland basin. A zone proximal to the thrust front (<150 km distance) exhibits high sediment accommodation and tectonic subsidence, probably due to Airy isostasy. In contrast, tectonic subsidence and sediment accommodation in a second zone located farther basinward (>150 km distance) decreases to the east, probably due to flexural subsidence across the ramp. The different subsidence modes significantly influenced stratal stacking and sequence boundary character throughout the history of foreland basin infilling. The U2-U3 (96.5-90 Ma) sequence in Figure 1 is an example of a composite sequence that formed due to regional loading and crustal relaxation. The U2 unconformity defines the top of the Lower Cretaceous basin fill (Stop 3.2 in Fig. 2). Overlying 3rd-order sequences of Late Cretaceous age are stacked into retrograding, aggrading, and prograding sequence sets (Stops 3.4, 3.5 in Fig. 2).

Thrust-loading also impacted short-term sediment accommodation and stratal patterns during final shortening in the latest Campanian, Maastrichtian, and early Paleocene (Schwans, 1987b; Lawton and Trexler, 1991; Talling et al., 1995). Movement along the foreland thrust systems (G and W in Fig. 3) caused segmentation of the proximal zone into a series of north-south elongate, thrust-cored anticlines (*see* Maastrichtian-Paleocene in Fig. 5). The history of the anticlinal uplifts is manifested in the basin fill of adjacent synclines in a series of unconformity-bounded, clastic wedges (U8-U9 and U9-U10 sequences in Fig. 1) that onlap the anticlinal structures (Stops 1.1, 1.2, 1.3, and 3.1 in Fig. 2).

LOWER CRETACEOUS BASIN FILL

Sequence Stratigraphy and Zonation

Figure 6 is a measured section of the earliest foreland basin deposits in the proximal zone (Stop 3.1 in Fig. 2). Schwans (1985a, 1986b, 1988a, 1988b) discusses the facies, demonstrates the character and regional extent of the bounding unconformities, and suggests a Barremian(?) through late Albian age for the U1-U2 sequence; Figure 1 shows only the upper portion of the sequence and unconformity U2. The

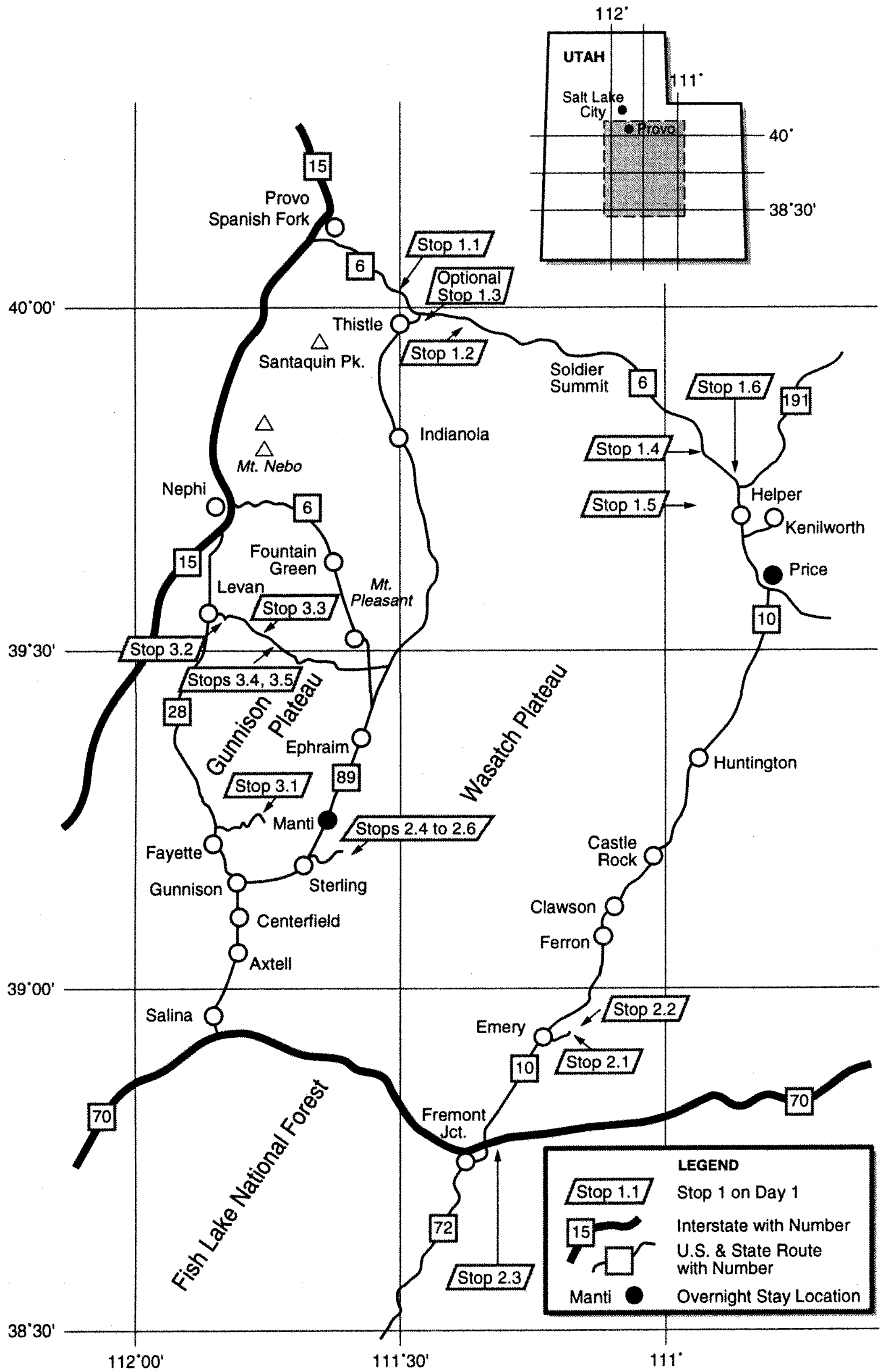

Figure 2. Location map of field trip area with stops and overnight stay locations indicated.

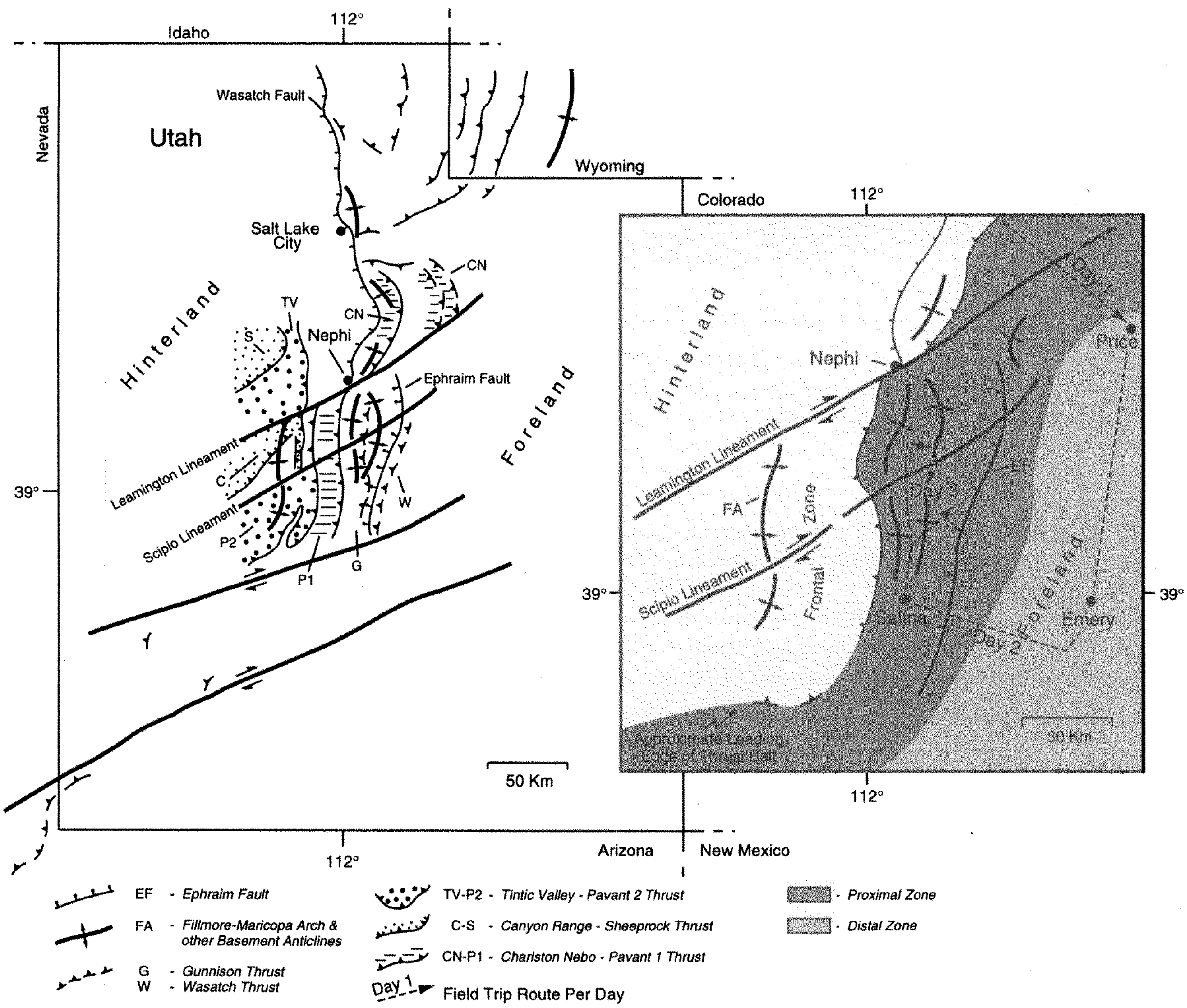

Figure 3. Map of the structural elements pertinent to foreland basin evolution in Utah. Modified after Allmendinger et al., (1986) and Picha (1986). The two shaded areas in the inset delineate the proximal and distal subsidence zones in the foreland basin; the approximate route of the field trip is shown for reference.

name Pigeon Creek Formation was suggested by Schwans (1988a) for the proximal clastics with the measured section in Figure 6 as the type section. Correlative formations are the Cedar Mountain and Burro Canyon formations in the distal zone in eastern Utah and western Colorado (Schwans, 1988b, which range in age from Barremian? through latest Albian (116.5-96 MA) (Heller and Paola, 1989; Yingling and Heller, 1992).

Proximal Zone Architecture

Initial sedimentation in the proximal zone and onset of thrusting occurred during Barremian through lower to middle? Aptian time and was marked by the deposition of *thin lacustrine limestones*, *flood plain mudstones*, and *intercalated channel-form sandstones* (*see* Lower Mbr. in Fig. 6). Floodplain-dominated systems were overwhelmed by *sheet-flood fan conglomerates* (Upper Mbr. in Fig. 6) during the middle? Aptian through late Albian. Fans were sourced by the emergent Pavant 1 allochthon and shed eastward and later southward into the subsiding foredeep (Schwans, 1986b, 1988a, 1988b). In the outcrop (Stop 3.1 in Fig. 2), earliest sheet-flood fan deposits are made up of thin sheets of *chert-pebble conglomerates and sandstones* set within thick sections of *variegated mudstones*. Later, fan deposits form a

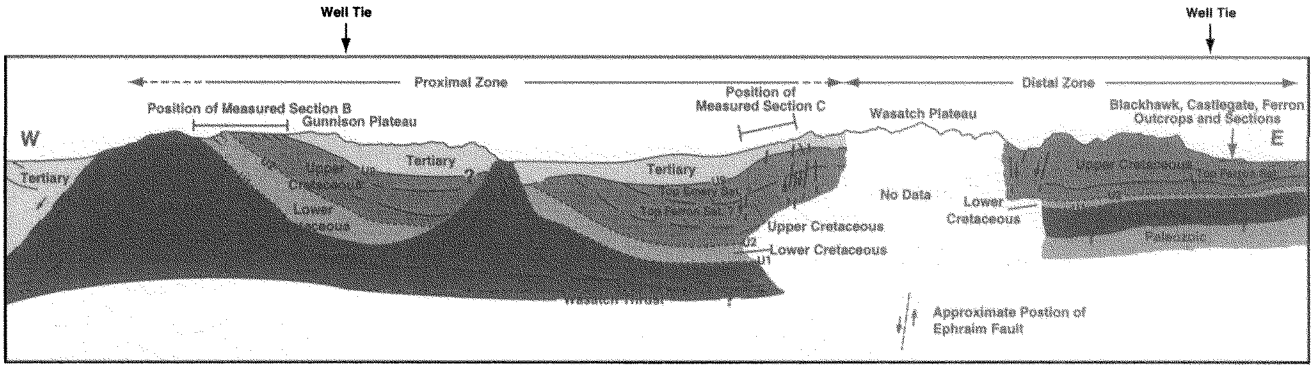

Figure 4. Interpreted seismic line and structural-stratigraphic cross section across the proximal and distal zones of the foreland basin margin. The interpretations are based on seismic tied to wells (see Well Tie), well-log correlations of Schwans (1988b, 1995), and outcrop data (see Position of measured section B, Blackhawk, Castlegate, Ferron Outcrops and Sections). No Data, refers to poor seismic data and no visible geometries.

thick succession of quartzite- and carbonate-clast *sheet-flood conglomerates* stacked into vertically amalgamated and laterally overlapping sheets separated by thin, *red mudstones* (Fig. 7). The succession of clast lithologies, clast sizes, and facies reflects hanging wall emergence and erosion of the Pavant 1 allochthon, resulting in an inverted clast-lithology stratigraphy (Schwans, 1998a).

Sediment thicknesses of the initial basin fill (e.g., Barremian through early to middle? Aptian) range from >300 m at the thrust front to 100 m along the eastern edge of the proximal zone (*see* dark grey area west of left dashed line, e.g. LPC, in Fig. 8). Sheet-flood fan accumulation was most pronounced in areas located basinward of the intersection point between the Leamington lineament and the frontal zone. The latter acted as a lateral ramp between the Charlston-Nebo thrust sheet to the north and the Pavant 1 thrust sheet in the south; the resulting tear fault zone between the thrust sheets formed a paleovalley and acted as sediment conduit. In contrast, sediment thicknesses during the middle? Aptian through late Albian range from >600 m at the thrust front to 300 m along the eastern edge of the proximal zone (*see* darkest grey area west of left dashed line, e.g. UPC, in Fig. 9) (Heller and Paola, 1989).

Distal Zone Architecture

Initial deposition in the distal zone in eastern Utah and western Colorado during the Barremian through lower-middle? Aptian consisted of chert- to quartzite-pebble conglomerates and sandstones transported in braided to low-sinuousity, multi-channel systems. Early drainages seem restricted to northwest-southeast oriented, broadly incised paleovalleys located in southeastern and eastern Utah (*see* light gray area, e.g. LBC and LCM, in Fig. 8) (Yingling and Heller, 1992). Well logs indicate that sediment thicknesses in the paleovalleys do not exceed 60 m (Schwans, 1986b, 1988b).

The coarse-clastic paleovalley fills are overlain by extensive *flood plain mudstones* with thin intercalated *lacustrine limestones, paleosols,* zones of calcrete nodules, and partially to completely exhumed, *highly sinuous, channel-form sandstones* with laterally attached *sheet sandstones.* The flood plain-dominated successions are of Albian-age and were deposited across a wide area of minor topographic relief that experienced little or no subsidence (*see* light and lightest grey area east of left dashed line, e.g. UCM and UBC in Fig. 9). Well logs indicate that sediment thickness does not exceed 300 m (Schwans, 1986b, 1988b).

Implications for Basin Subsidence

Initial basin subsidence in the proximal zone allowed the accumulation of 1000 m of strata within a narrow subsiding trough defined by the Pavant 1 thrust front in the west and the Ephraim Fault in the east. Conversely, sediment accommodation in the distal zone during the same time interval was more or less insignificant across a wide basin area. Schwans (1986b, 1987a) interpreted this difference in sediment accommodation patterns to indicate that tectonic subsidence in the proximal zone was predominantly an Airy isostatic subsidence of basement blocks beneath and near the thrust load and de coupled or detached from subsidence of the stable, unbroken craton of the distal zone. A comparison of Figures 8 and 9 shows that net aggradation and net subsidence accelerated during the late Aptian through Albian, involving most of eastern Utah. This change is interpreted to reflect the change from laterally restricted, Airy isostatic subsidence near the load to larger scale, flexural subsidence.

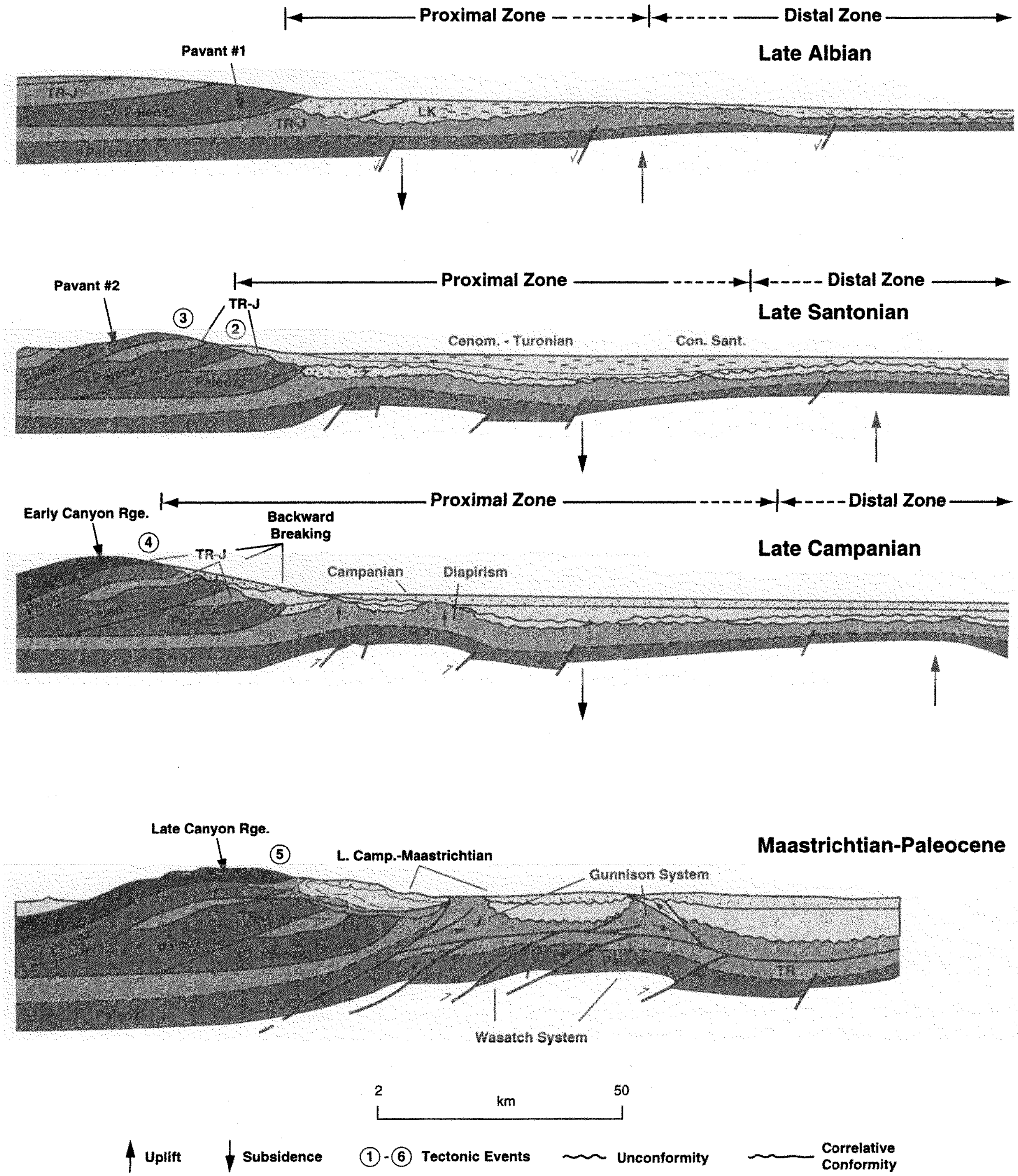

Figure 5. Interpreted compressional history of the Cretaceous fold-thrust belt in central Utah. Structural relationships and timing after Villien and Kligfield (1986) and Schwans (1988a, 1988b).

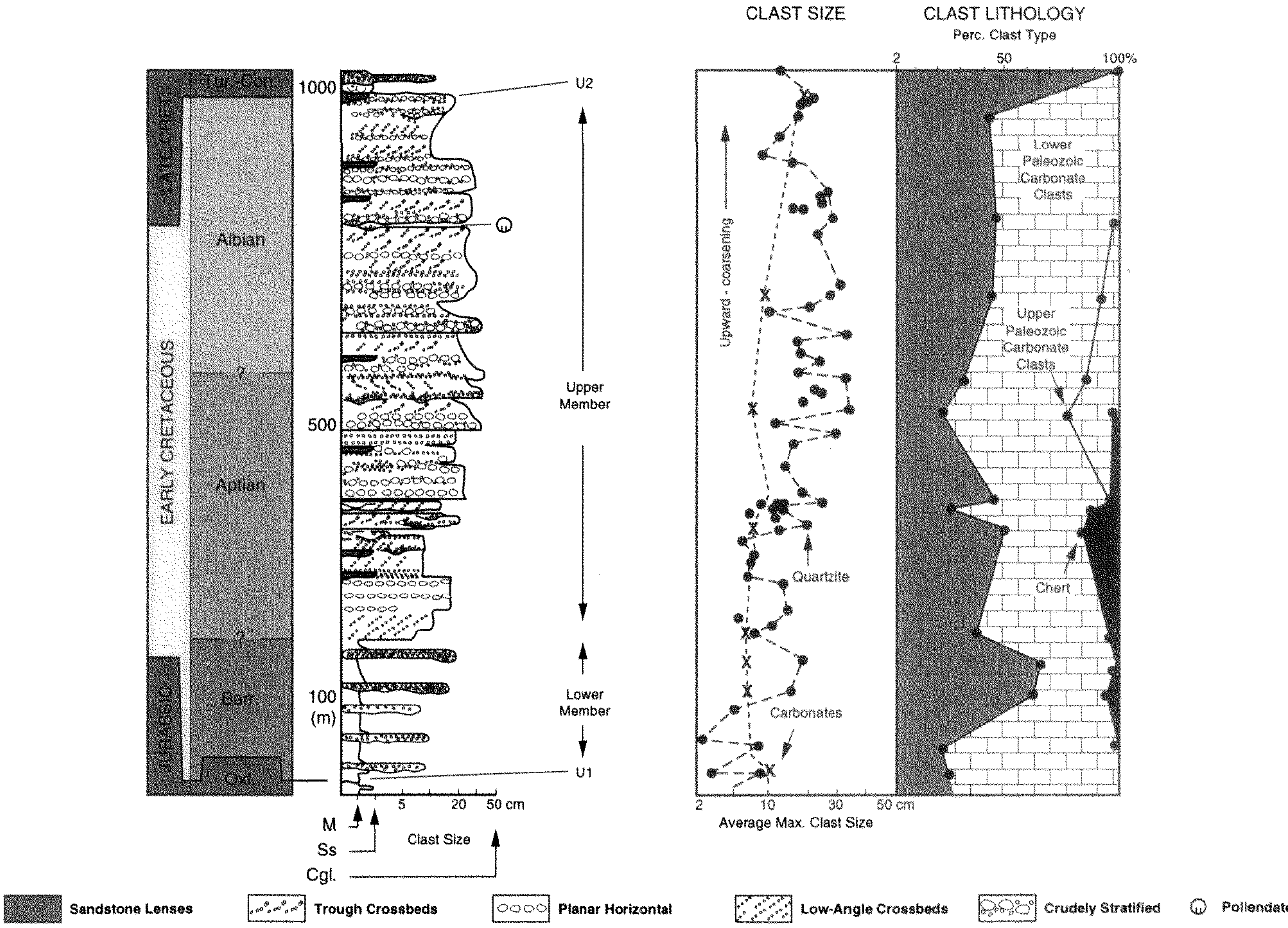

Figure 6. Measured section of the Lower Cretaceous portion of Indianola Group (Undifferentiated) of Spieker (1946, 1949) in Chicken Creek Canyon (Sec. 12, T. 15S, R. 1E), east of Levan, Utah (Stop 3.2 in Fig. 2). The section shows the age, grain size distribution, bedding types, maximum clast size distribution, and clast type distribution for the Pigeon Creek Formation of Schwans (1988a, 1988b). The section defines the U1–U2 sequence of Figure 1.

UPPER CRETACEOUS SEQUENCE BASIN FILL

Sequence Stratigraphy and Zonation

Spieker (1946, 1949) defined the Upper Cretaceous Indianola Group and its members (*see* Proximal Foreland column in Fig. 1). Lawton (1982, 1983) presented an updated lithostratigraphic framework and facies scheme. Schwans (1985b, 1986a, 1988b, 1989, 1990, 1991, 1995) revised the biostratigraphy and proposed a sequence-stratigraphic framework for the Upper Cretaceous Indianola Group (*see* Proximal Zone in Formation Stratigraphy column in Fig. 1) and associated time-equivalent units, including conglomerates to the west in the Gunnison Plateau (*e.g.*, Indianola Group [Undifferentiated] of Spieker [1946, 1949]), the Canyon Range, and in the Pavant Range (*e.g.*, Hinterland column in Fig. 1), as well as shallow-marine strata in the east in the Wasatch Plateau and Book Cliffs (Distal Foreland column in Fig. 1).

Nine unconformities and ten depositional sequences (U2 through U10 in Fig. 1) are identified in the basin fill. Within each depositional sequence alluvial fan conglomerates and braided stream sandstones located at the thrust front (Figs. 10, 11) grade down-depositional dip and eastward into braided stream and overbank successions (Figs. 12, 13) (Stops 3.1, 3.4, 3.5 in Fig. 2); the latter may be cut by conglomeratic valley fills several kilometers wide and up to 300 m thick (*see* conglomerates in measured sections Figs. 11, 12, 14) (Stops 3.4, 3.5, and Optional Stop 1.3 in Fig. 2). The nonmarine strata give way to shoreline and open-marine facies via wave-dominated shorelines (Stop 1.5 in Fig. 2), fluvial-dominated deltas (Stop 2.1, 2.2 in Fig 2), and braid-deltas (Figs. 15, 16) (Stops 2.4, 2.5., 2.6 in Fig. 2).

Figure 7. Photograph of sheet-flood conglomerates *with intercalated thin,* red mudstones *at Stop 3.2 (Fig. 2). The strata are part of the Upper Pigeon Creek Member of Schwans (1988a).*

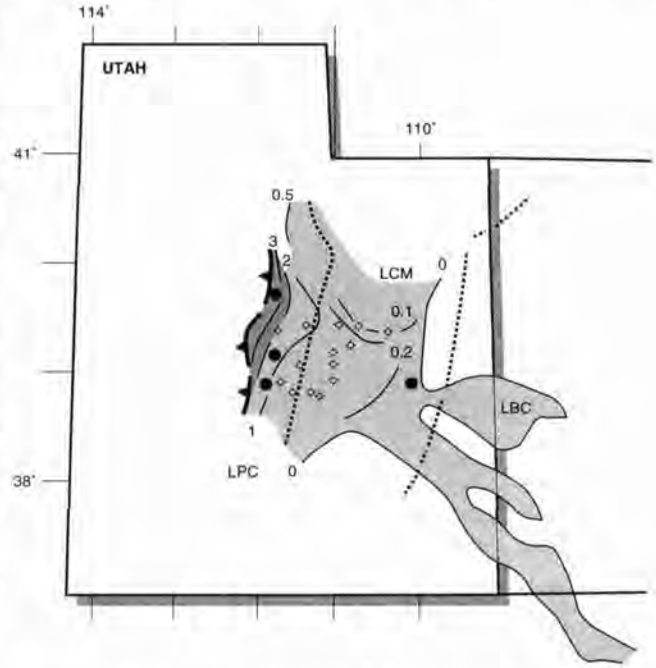

Figure 8. Thickness distribution of Barremian through middle Aptian strata in Utah. Thicknesses are in hundreds of meters and based on measured sections (heavy dots) and interpreted well logs (well symbols) from Schwans (1988b). The shading highlights the thickness variations. Dashed line between LPC (Lower Pigeon Creek Formation) and LCM (Lower Cedar Mountain Formation) depicts the eastern limit of the proximal zone; dashed line between LCM and LBC (Lower Burro Canyon Formation) depicts approximate eastern limit of distal zone.

Three types of sequences and sequence boundaries are observed: (1) high-frequency sequences and unconformities with probable cyclicities of 100,000–200,000 years; (2) third-order sequences and unconformities with cyclicities of about 1–3 MY.; and (3) composite sequences and unconformities with cyclicities greater than 3 MY.; composite unconformities consist of several, merged higher frequency surfaces. Examples for the first type are the high-frequency sequences and unconformities observed in the Dakota Formation and the U4 surface in Figure 1, which separates the upper and lower Ferron Sandstone of Schwans (1988b, 1995) (Stop 2.3 in Fig. 2). The surfaces and strata record the numerous changes in relative sea level during the gradual westward shift of shoreline facies across Utah with the incursion of the seaway in the late Albian through early Turonian. Likely examples of third-order sequences and unconformities and probably the direct result of eustasy in the marine foreland basin and (Type-1 sequences *in sensu* Van Wagoner et al., 1990) are the surfaces U3 and U6 in Figure 1 (Stop 2.3, 2.6, respectively in Fig. 2). The third type, composite sequences and unconformities, seem to be most common in the foreland basin fill; examples are the surfaces U2 (Stop 3.2 in Fig. 2) and U8 through U10 (Stops 3.1, 3.4, and 1.4 in Fig. 2). These types of unconformities are marked angular toward the tectonic belt and exhibit a variable hiatus (Figs. 4, 10, 12). An example is the U2 surface and its associated hiatus, which may span as much as 5 MY. at the thrust front and as little as 0.25–3 MY. in the distal zone. This variation is interpreted as the combined result of erosion and sediment bypass, following thrust emergence and westward directed onlap with basin subsidence and seaway expansion. Figure 17 (Stop 3.1 in Fig. 2) is an example of a composite surface associated with local uplift and infilling of the adjacent sub basin; the hiatus associated with this surface may range from < 5 MY. in the basin to > 10 MY. on structure (Schwans, 1987b, Talling et al., 1995).

Proximal Zone Architecture

Individual depositional sequences in the proximal zone are defined by a spectrum of depositional environments, which includes, arranged from up-dip to down-depositional dip, alluvial fan deposits, conglomeratic paleovalley fills, and braided stream deposits. Table 1 summarizes the lithofacies and interpreted depositional environments in the proximal zone.

Alluvial fan clastics are the most proximal deposits found in the Upper Cretaceous basin fill (Figs. 10, 11). Figure 11 shows crudely stratified *block and boulder conglomerates* and cross bedded *scour-based boulder- to cobble-conglomerates* forming 20 m to 30 m-thick, upward-fining successions. The successions in turn stack to form 500 m to 1000 m

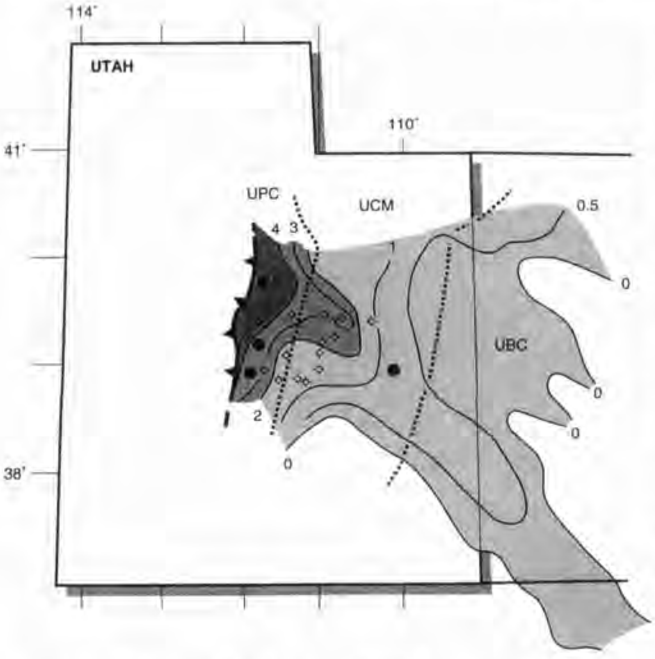

Figure 9. Thickness distribution of Middle Aptian through late Albian age strata in the foreland basin in Utah. Thicknesses are in hundreds of meters and based on measured sections (heavy dots) and interpreted well logs (well symbols) from Schwans (1988b). The shading highlights the thickness variations. Dashed line between UPC (Lower Pigeon Creek Formation) and UCM (Upper Cedar Mountain Formation) depicts eastern limits of proximal zone; dashed line between UCM and UBC (Upper Burro Canyon Formation) depicts approximate eastern limit of distal zone.

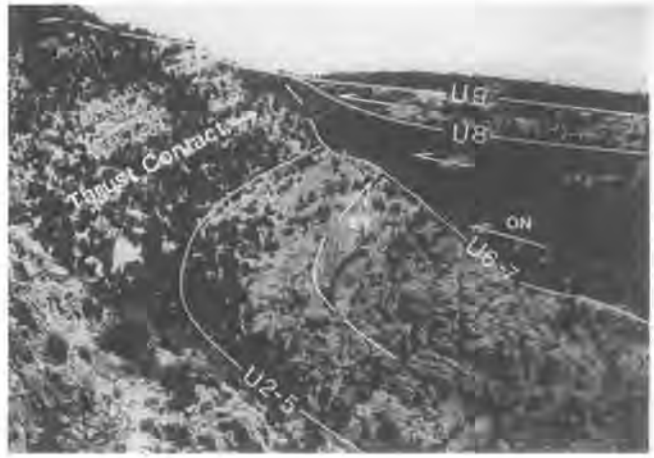

Figure 10. Photograph of alluvial fan conglomerates and braided stream sandstones located at the thrust front in Oak Creek Canyon in the Canyon Range (see measured section A in Fig. 11). Canyon Range thrust (arrow) and position of unconformities are indicated. ET–erosional truncation; ON–onlap.

wide, wedge-shaped stratal bodies. The *block and boulder conglomerates* occur at the thrust front in the Canyon and Pavant ranges and are interpreted by Schwans (1988b) to represent alluvial fan deposition by catastrophic, bedload-concentrated flows transported during episodic flood discharges under a humid-tropical climate; overlying finer grained *cross bedded pebbly sandstones* represent low-energy deposition on the fan surface, possibly during lower water stage in small channels and bars. The measured section shown in Figure 11 is located west of the field trip area in the Canyon Range (Figs. 3) and will not be visited; it is shown here to provide a more complete depositional spectrum.

The *scour-based boulder- cobble-conglomerate* and *gravely sandstone* facies association is the coarsest in the field trip area and forms discrete paleovalley fills that are several kilometers wide and 50–250 m deep (Stops 1.2, 3.4 in Fig. 2). Examples are the strata above U7 in Figures 12 and 14 (Stop 3.4 in Fig. 2) and the incised valley fill above U3 in Figure 16 (Optional Stop 1.3 in Fig. 2). The strata are part of the Indianola Group (Undifferentiated) of Spieker (1946, 1949) and correspond to the Reddicks Canyon Conglomerate and the Lower Funk Valley Sandstone of Schwans (1988b) in Figure 1. Transportation and deposition of conglomerates occurred in shallow bars under a perennial and seasonally wet-tropical climate; interbedded lenses of gravely sandstones are the fills of small channels.

The bedload to mixed load braided stream deposits comprise the bulk of the Upper Cretaceous coarse-clastics, formerly called Indianola Group (Undifferentiated), in the proximal foreland zone. Lithofacies of these deposits are arranged into 150–300 m-thick upward-fining, sheet-like bodies that parallel the structural strike of the frontal zone for 10 km to > 100 km. In the measured section in Figure 12, the lower, coarse-clastic portion of individual upward-fining units are trough cross-bedded, *scour-based, cobble-pebble conglomerates* of sheet geometry grading upward into cross bedded, *pebbly sandstones* and *sandstones* (e.g., strata immediately above U3, U4, U5, and U6 in Fig. 12) (Stop 3.3 in Fig. 2). Conglomerates and sandstones were transported and deposited in mixed gravely and sandy bars in a braided stream. The coarse clastics of individual upward-fining units are overlain along a sharp surface by a thick section of *overbank siltstones* and *detrital carbonates* with a wide variety of ripple cross-stratification, an abundance of secondary sedimentary structures, and numerous angiosperm leaf impressions (Schwans, 1988b). Intercalated are trough cross bedded, *pebbly channel-form sandstones* (Stop 3.3 in Fig. 2). This facies association is interpreted to represent mixed sand-mud deposition by low-sinuosity channels located in a ponded flood plain.

Figure 13 is a composite photo of a portion of the measured section in Figure 12. Figure 18 is a block diagram

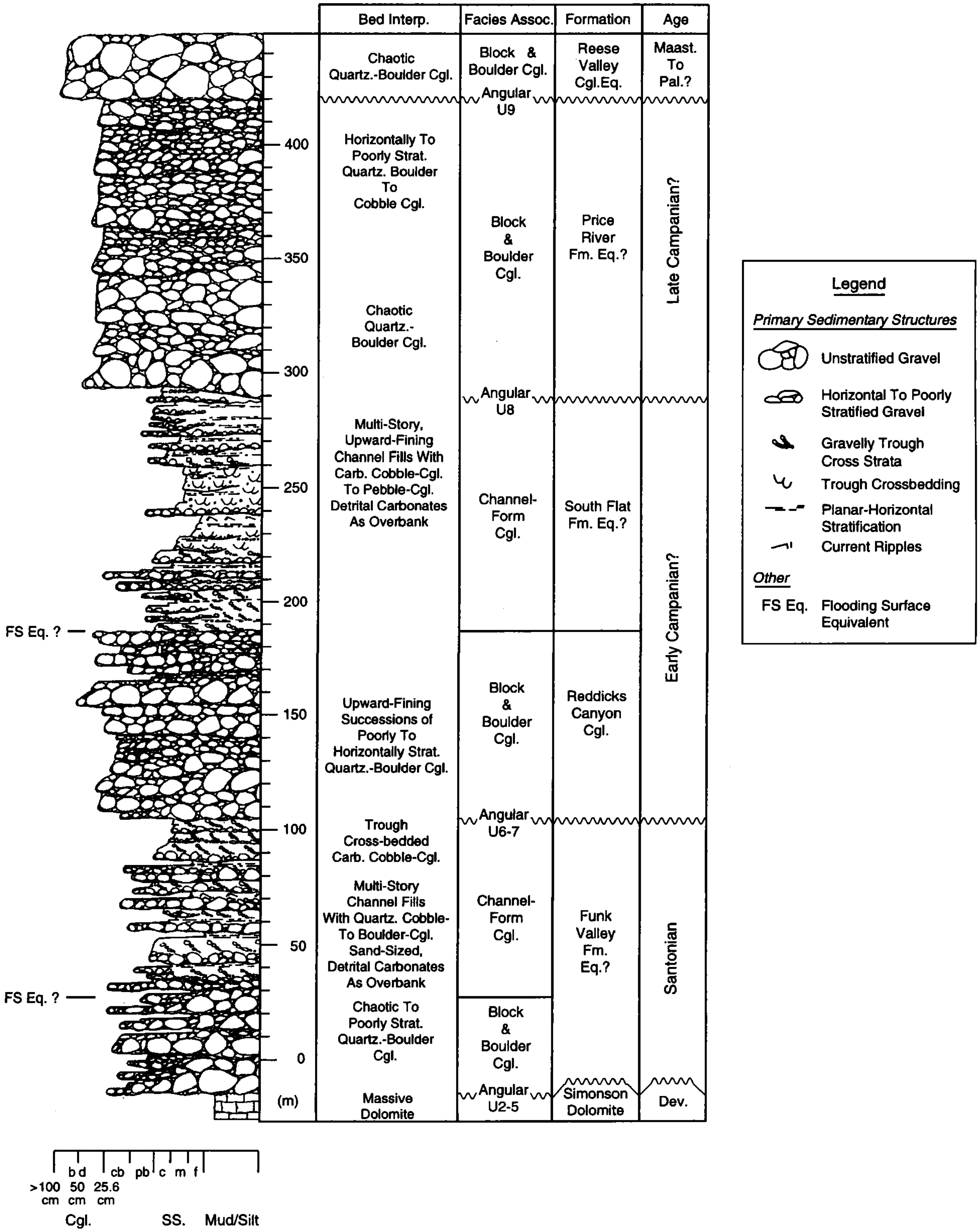

Figure 11. Measured section A of alluvial fan conglomerates shown in Figure 10. Section was measured in Oak Creek Canyon (Sec. 10, T. 17S., R. 2W.), Canyon Range, Utah. Lithofacies include crudely stratified block and boulder conglomerates, *cross bedded* scour-based boulder- to cobble-conglomerates, *and* cross bedded pebbly sandstones *arranged into 20 m to 30 m-thick, upward-fining successions.*

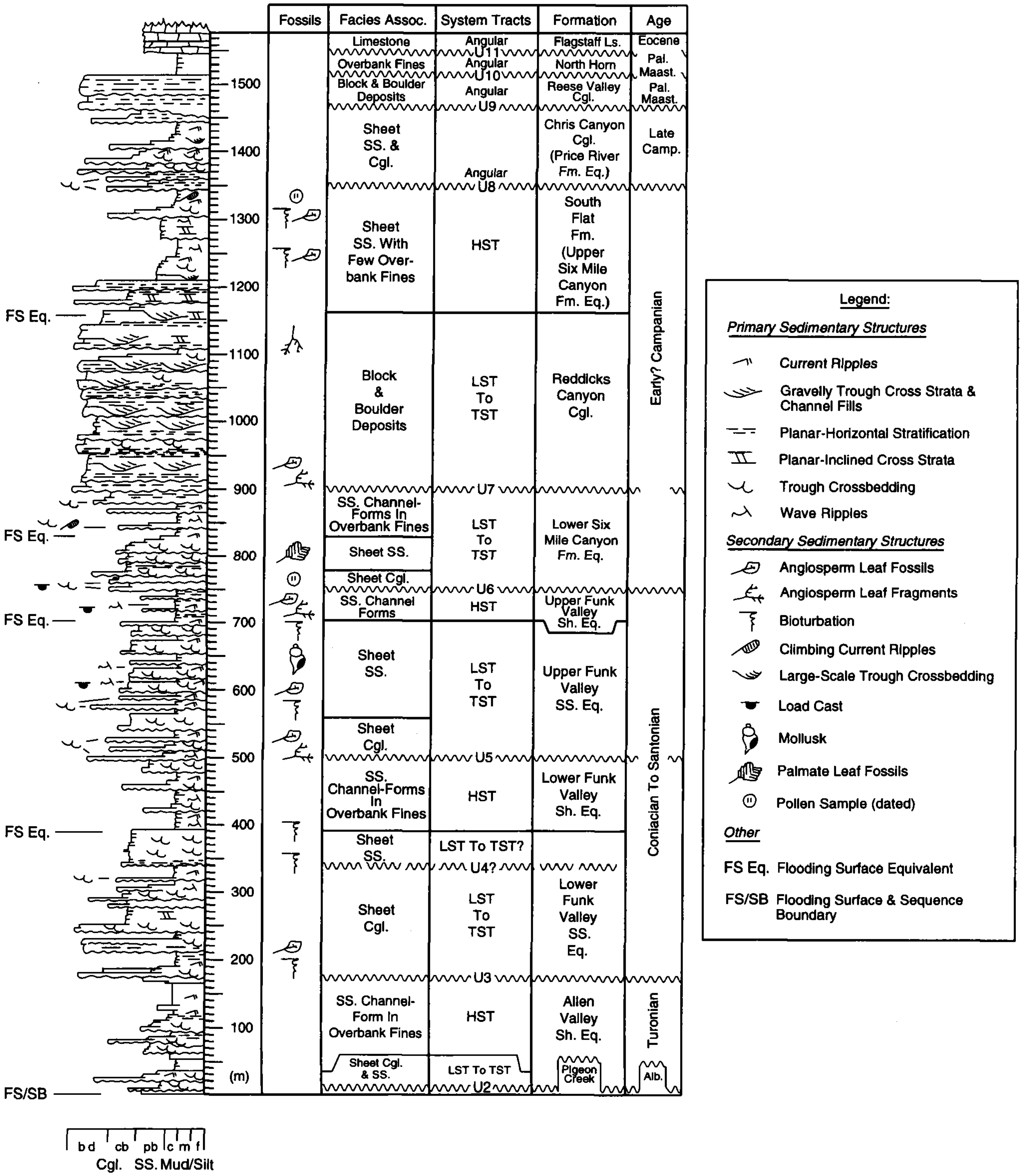

Figure 12. Measured section B (see Figs. 1 and 4) of the Upper Cretaceous portion of the Indianola Group (Undifferentiated) of Spieker (1946, 1949) in Chicken Creek Canyon (Sec. 12, T. 15S, R. 1E), east of Levan, Utah (Stops 3.2 through 3.5 in Fig. 2). The section illustrates the alluvial architecture of ten depositional sequences of Schwans (1988b, 1995).

Figure 13. Composite photograph of three depositional sequences shown in Figure 12 (Stops 3.4, 3.5 in Fig. 2). Within each sequence the coarse-clastic braided stream deposits represent the lowstand to transgressive systems tract (LST-TST), while overlying overbank fines with intercalated single-channels forms are the highstand systems tract (HST). Strata dip to the left and east, view is to the south. ET–erosional truncation; ON–onlap.

that illustrates sequence architecture and sequence stacking for nonmarine strata in the proximal zone. According to Schwans (1995), each large-scale, upward-fining unit is a depositional sequence bounded by unconformities. Within each sequence the coarse-clastic braided stream deposits represent the lowstand to transgressive systems tract (LST-TST in Figs. 1, 12), while overlying overbank fines with intercalated channels form the highstand systems tract (HST in Figs. 1, 12). The systems tracts in the proximal zone are thus defined by a change in depositional architecture from a bedload-dominated, fluvial systems with vertically amalgamated channels to a suspended-load dominated system with isolated channel-forms set in overbank fines.

Distal Zone Lithofacies And Architecture

Individual depositional sequences in the distal zone include a range of depositional environments; these are fluvial-dominated shoreline deposits, wave-dominated shoreline deposits, and open-marine deposits. Table 2 summarizes the lithofacies and interpreted depositional environments in the distal zone.

Fluvial-dominated shoreline deposits are exposed along the western (Stops 2.4, 2.5, 2.6 in Fig. 2) and eastern margins (Stops 2.1, 2.2, 2.3 in Fig. 2) of the Wasatch Plateau, or proximal and distal zones, respectively, and feature coarse-grained *tabular sandstones* and finer grained *lenticular sandstones* separated by thick *mudstones with thin beds of siltstones and muddy sandstones*. In the measured section in Figure 15, *tabular sandstones* exhibit low-amplitude cross beds, numerous reactivation and internal scour surfaces, and abundant shelly debris. This 50 m-thick section above unconformity U3 is part of the Lower Funk Valley Formation of Schwans (1988b) and reflects braid-delta progradation into a shallow-marine, estuarine embayment and shallow-incised paleovalley. The sandstone bodies onlap U3 along depositional strike (Fig. 19) and form a part of the lowstand to transgressive systems tract above U3 (LST to TST in Figs. 1, 15). The shales beneath U3 are part of a highstand systems tract (HST in Figs. 1, 15) and form the Allen Valley Shale of Spieker (1946, 1949) (Stop 2.4 in Fig. 2).

The *tabular sandstones* are sharply overlain along a flooding surface (first FS above U3 in Fig. 15) by a 250 m-thick interval of *mudstones with thin beds of wave- and flaser-rippled siltstones and muddy sandstones* organized into 10–15 m-thick, coarsening-upward parasequence sets; the latter are crevasse splays and small deltas that shed into brackish-water bays. Parasequences feature mudstones and siltstones coarsening upward into rippled, often soft-sediment deformed, bioturbated, muddy sandstones with lags of mollusks. The deposition of the mudstone-dominated interval occurred in response to a rise in relative sea level during early highstand systems tract (Schwans, 1995) (HST above U3 in Figs. 1, 15).

Lenticular sandstones, shelly banks, and mudstones are common in the distal zone at the eastern margin of the Wasatch Plateau (Stops 2.1, 2.2, 2.3 in Fig. 2). Mudstone-siltstone intervals feature a variety of ripple cross strata (*see* Table 2), normal-graded beds, and burrows, and coarsen

Figure 14. Photograph of the incised paleovalley fill located above U7 in Figures 12 and 13 (Stop 3.4 in Fig. 2). The paleovalley fill is the Reddicks Canyon Cgl. of Schwans 1988b (see Figs. 1, 12). Strata are dipping to the east (top of photo). Note the flat lying Tertiary strata above U9 and U10.

upward into sandstones with low-angle inclined laminae sets (Stop 2.1). In places, zones with tightly packed shell fragments and whole pelecypod valves occur. Symmetrical channel scours up to 4 m wide and 2 m deep are cut into the tops of the sandstone bodies. The lithofacies stack to form a series of deltaic parasequences and parasequence sets of the inner and outer stream-mouth bar. Figures 20 and 21 show an example of two such deltas (Stop 2.3 in Fig. 2). The photos show the Coniacian-age, Upper Ferron Sandstone of Schwans (1988b, 1995) and Cotter (1971, 1975) and represent fluvial-deltaic progradation in the distal zone during the lowstand to transgressive systems tract above unconformity U4 (Fig. 1). The Coniacian age designation and formation interpretation is contrary to that of Gardner (1993), Ryer (1981) and Ryer and McPhillips (1983). Schwans (1988b, 1995) offers a detailed discussion of the biostratigraphy, well-log correlations, and paleogeographic reconstructions. Figure 22 is an outcrop and well-log cross section excerpted from Schwans (1995) and illustrates the stratal relationships between the Lower Funk Valley Sandstone exposed in measured section C (Stop 2.4 and Fig. 15) in the proximal zone and the Upper Ferron Sandstone exposed in Stops 2.1 through 2.3 in the distal zone (Fig. 2). In the cross section the unconformity U4 truncates most of the underlying Lower Ferron Sandstone of Turonian age toward the east and superposes Coniacian-age, fluvial-deltaic strata of the Upper Ferron onto pro delta and offshore mudstones of the Turonian-age Lower Ferron, indicating a significant basinward shift in facies and the presence of U4 in Stop 2.3 (Fig. 2). The parasequence set stacking pattern observed in said stops is also present in the nearby wells. For example, the lower flooding surface (*e.g.*, FS above U4 in Figs. 20, 21) that separates the two stacked deltas and parasequence sets in the outcrop can be correlated to the flooding surface that separates the upper and lower sand above U4 in wells #3 through #5 in Figure 22. The delta-front clinoforms beneath the lower FS in the outcrop are truncated along their tops by channels of the inner stream-mouth bar, suggesting a high-frequency unconformity; the latter surface is marked also in the well-log cross section.

Wave-dominated shoreline deposits are found in the proximal zone at the western margin of the Wasatch Plateau (Stops 2.5, 2.6 in Fig. 2), where they form the Upper Funk Valley Sandstone of Schwans (1988b, 1995) (*see* strata above and below U5 in Figs. 15, 23), and in the distal zone at the eastern margin of the plateau, where they form the stacked shoreface units of the Blackhawk Formation (Stops 1.5, 1.6 in Fig. 2). Shoreline parasequences consist of *wave-rippled mudstones, siltstones, and sandstones* at their base that represent deposition at shelfal depth. These grade upward into *hummocky cross-stratified* and bioturbated, *trough cross-bedded sandstones* deposited by traction currents in the lower and upper shoreface; burrows are of the *Skolithos* ichnofacies. Parasequences in the proximal zone may exhibit *scour-based, pebbly sandstones* at their tops that have cut into underlying cross strata (*for example*, at 1390 m in Fig. 15).

Open-marine, fine-grained deposits are found in the proximal zone at the western margin of the Wasatch Plateau (Stops 2.4, 2.5, 2.6 in Fig. 2), where they form the Allen Valley Shale, the Lower Funk Valley Shale, and the Upper Funk Valley Shale of Schwans (1988b, 1995) (Figs. 1, 15, 19, and 23), and in the distal zone at the eastern margin of the plateau, where they form the Tununk and Bluegate tongues of the Mancos Shale (Stops 2.1, 2.2, 2.3 in Fig. 2). Open-marine deposits comprise thick intervals of massive to *horizontal-planar bedded, carbonaceous mudstones* with thin beds of *wave-rippled sandstones and flaser bedded siltstones to very fine sandstones*. Less common are thin, dark gray, foraminifer-bearing *micritic limestones*. Bioturbate structures indicate low species diversity and include small burrow of *Teichichnus sp.* and *Planolites sp.* Mudstones represent deposition in a distal pro-delta and shelfal setting at water depths below effective wave base and are deposited during the highstand systems tract of individual sequences (HST's in Fig. 1). The micritic limestones in the same interval are rare and probably reflect maximum water depth. Schwans (1988b) offers a detailed discussion of the fauna and biostratigraphy of the various Mancos tongues shown in Figure 1.

In the measured section in Figure 15, the deltaic and estuarine sandstones of the lowstand to transgressive systems tracts above U2 and U3 are abruptly overlain along a maximum flooding surfaces (MFS) by open-marine mud-

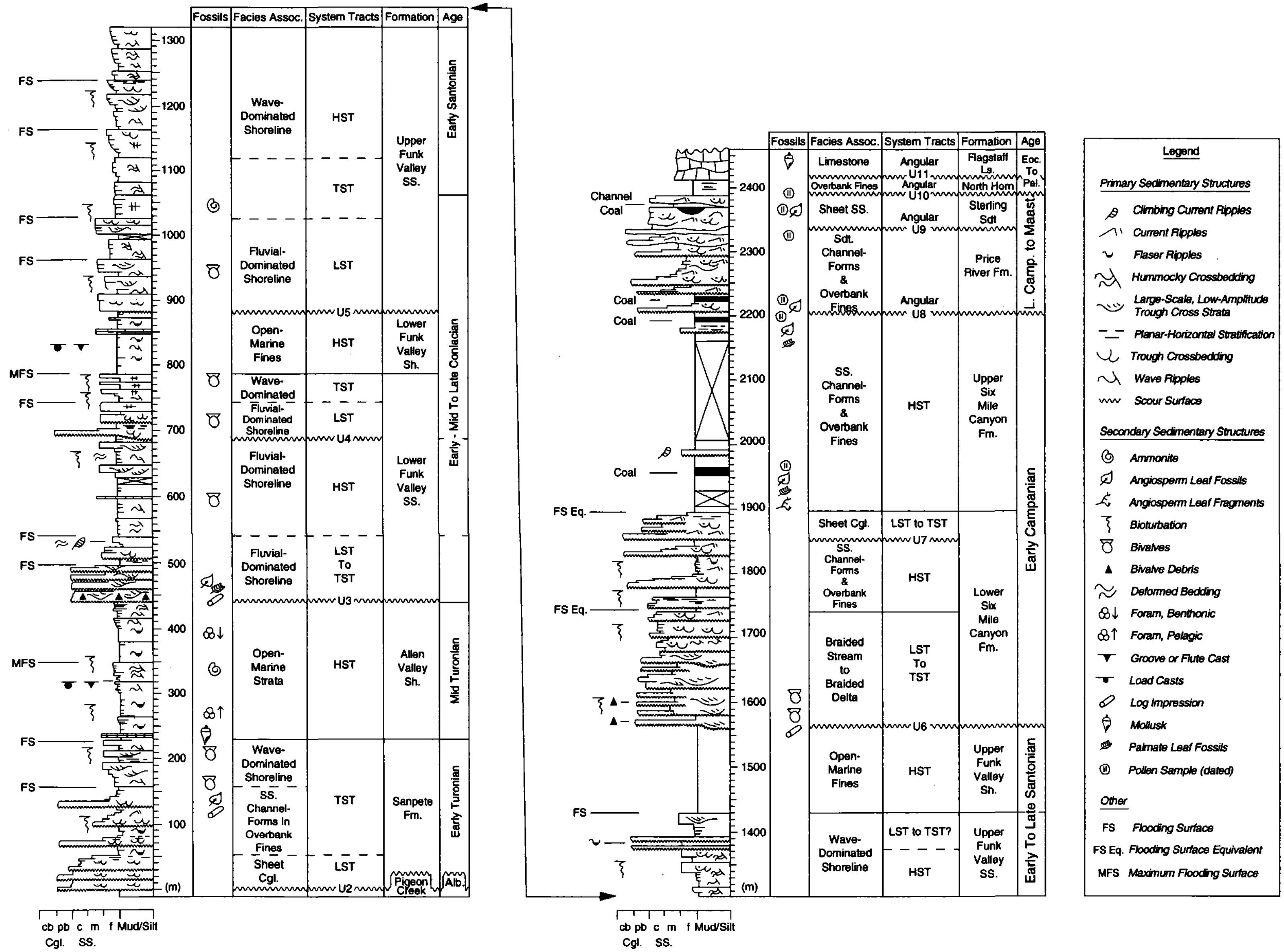

Figure 15. Measured section C (see Figs. 1, 4) of the Upper Cretaceous portion of the Indianola Group of Spieker (1946, 1949) at Palisade Lake State Park (Secs. 36-36-25, T. 18S., R. 2E.), east of Sterling, Utah (Stops 2.4 through 2.6 in Fig. 2). The section illustrates the alluvial to nearshore-marine architecture of ten depositional sequences of Schwans (1988b, 1995).

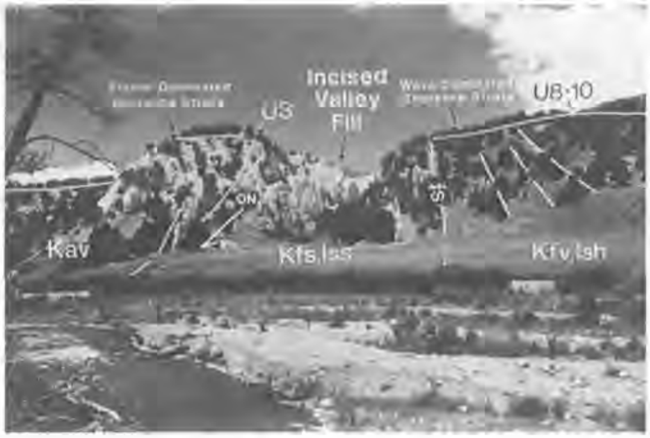

Figure 16. Photograph of an incised paleovalley fill (Optional Stop 1.3 in Fig. 2) equivalent to the Lower Funk Valley Sandstone (Fig. 1) at Lake Fork (Sec. 2, T. 9S., R. 4E.); strata are vertical and unconformably overlain along U8-10 by Paleocene-age Red Narrows Conglomerate (Fig. 1). Fluvial-dominated shoreline strata beneath U3 (e.g. to the left) are Early Turonian and equivalent to the Allen Valley Shale (Fig. 1). They are sharply overlain along a flooding surface (FS) by wave-dominated shoreline strata of the transgressive systems tract of middle-late Turonian age, based on mollusks described in Schwans (1988b).

Figure 17. Photo of an uppermost Maastrichtian to Eocene piggyback basin fill in Mellor Canyon (Stop 3.1 in Fig. 2), near the town of Fayette (Sec. 17, T. 18S., R. 1E.), southwestern Gunnison Plateau. The Tertiary-age, deformed conglomerates and overbank mudstones of the North Horn Formation and the lacustrine limestones of the Flagstaff Limestone onlap probably Campanian-age, east-dipping (e.g. to the right), braided stream deposits of the Six Mile canyon Formation along composite surface U8-9. View is to the north. ET–erosional truncation; ON–onlap.

stones of the corresponding highstand systems tract. The highstand strata are truncated by the sequence boundaries, which are overlain by fluvial-deltaic, incised-valley deposits of the next lowstand systems tract (*see* strata above U3 through U6 in Figs. 19, 23), indicating repeated relative shallowing of the basin and a basinward shift in facies. Figure 24 is an example of a significant basinward shift in facies across U6 (Fig. 15), superposing braided-stream conglomerates of the lowstand systems tract onto open-marine mudstones of a highstand systems tract.

CONCLUSIONS

The facies architecture and the associated parasequence and sequence stacking patterns across the foreland basin margin occur within an accommodation cycle of subsidence and sea level change. Case I in Figure 25 shows the architecture and stacking patterns for a period marked by high tectonic subsidence (*e.g.*, proximal zone), multiple higher frequency changes in relative sea level, and abundant sediment supply. The fluvial architecture of a highstand systems tract in the sea level cycle shown (1 and 3 in case I of Fig. 25) is marked by overbank-dominated systems with well-defined, single-channel geometries. Correlative nearshore-marine strata show an aggradational parasequence stacking pattern. The associated lowstand systems tract (2 in Case I) is characterized by a change in parasequence stacking pattern from aggradational to progradational and a minor basinward shift in facies. At the same time, fluvial architecture in the up-dip shows increased channel clustering to lateral coalescing of single-channel geometries. Examples for Case I stacking patterns and architecture are the Emery Sandstone and the correlative Upper Funk Valley Sandstone (U5-U6 sequence in Fig. 1).

Case II in Figure 25 shows the architecture and stacking patterns for a period marked by low tectonic subsidence (*e.g.*, distal zone) and multiple higher frequency changes in relative sea level under an abundant supply of sediment. As was previously the case, the fluvial architecture of a highstand systems tract (1 and 3 in case II of Fig. 25) is marked by overbank-dominated systems with single-channel geometries and correlative nearshore-marine strata are essentially aggradationally stacked. The associated lowstand systems tract, however, is marked by an abrupt change in parasequence stacking pattern from aggradational to progradational, a major basinward shift in facies, subaerial erosion of marine strata, and formation of incised valley systems. Correlative fluvial architecture in the up-dip shows formation of bedload-dominated systems and valley incision. Examples for Case II stacking patterns and architecture are the Ferron Sandstones and the correlative Lower Funk Valley Sandstone (U3-U4 and U4-U5 sequence in Fig. 1) and the Blackhawk and Six Mile Canyon formations (U6-U7 sequence in Fig. 1).

The described accommodation cycle of subsidence and sea level change can be applied to characterize and predict depositional architecture per basin zone and sequence.

Table 1: Lithofacies and depoitional environments in the proximal zone

Environment	Lithofacies & Bedding Types
Alluvial Fan	*Block and boulder conglomerates* • chaotic to crude-horizontal stratification *Scour-based, boulder-cobble-pebble conglomerates and gravely sandstones* • trough cross beds, horizontal planar beds, ripple cross beds
Paleovalley Fills	*Scour-based, boulder-cobble conglomerates and gravely sandstones* • low-angle, planar-inclined cross beds, trough cross beds, horizontal planar beds
Bedload to Mixed-Load Braided Stream	*Scour-based, cobble-pebble conglomerates, pebbly sandstones, and sandstones* • trough cross beds
Mixed to Suspended Load Fixed-Channel Stream and Floodplain	*Pebbly, channel-form sandstones* • trough cross beds *Overbank siltstones, mudstones, and detrital carbonates* • trough cross beds, ripple cross beds, contorted beds, load and flute casts, rizoliths, biogenic traces of *Scoyenia* ichnofacies, angiosperm leaf impressions

Facies successions are thus not only specific to either foreland basin zone, but are also definitive with respect to the changes in the position of relative sea level and can be grouped into the three component systems tract.

ROAD LOG

(Refer to Figure 2 for Stops, town names, and landmarks)

Day 1

Key Topics: Thrust systems and basin-fill overview; alluvial fan facies, braided stream facies (Flagstaff Ls., Red Narrows Cgl., North Horn Fm., Price River Fm., Castlegate Sdst.) wave-dominated shoreline facies (Blackhawk Fm.); parasequence expression and stacking patterns; unconformity types.

Miles

0.0 Travel south on I-15 from Salt Lake City to Provo. Interstate runs parallel to the Wasatch Mountains. The Wasatch Fault, a major down-to-the-west normal fault, lies at the base of the foothills of the Wasatch Range.

50.0 Exit I-15 onto Routes 89 and 6 proceed on Route 6 toward Price.

56.0 The road approaches the Wasatch Mountains and passes through Pennsylvanian to Permian marine sedimentary rocks.

64.0 **Stop 1.1—Charlston-Nebo Thrust at summit at Lake Fork.**
Jurassic Navajo Sandstone of the Charlston-Nebo thrust allochthon is exposed on north side of highway cut. Individual trough cross sets are up to 50 m thick. The Navajo Sandstone is conformably overlain by the Jurassic Twin Creek Limestone. The rocks are part of the platform assemblage deposited prior to Cretaceous thrusting and foredeep development.

65.0 **Stop 1.2—Red Narrows Conglomerate, Late Maastrichtian?-Paleocene, Lake Fork**
The Red Narrows conglomerates form the basal portion of a piggy-back basin fill; the basin formed and detached along the Gunnison and Wasatch thrusts during the latest Maastrichtian (Fig. 2). Conglomerates are part of the *scour-based, boulder-cobble conglomerates and gravely sandstones* facies association (*see* Table 1) and are sourced from the Triassic-Jurassic strata exposed in the Charlston-Nebo allochthon to the west. Conglomerates are in unconformably overlain and onlapped along unconformity U10 by the Paleocene North Horn Forma-

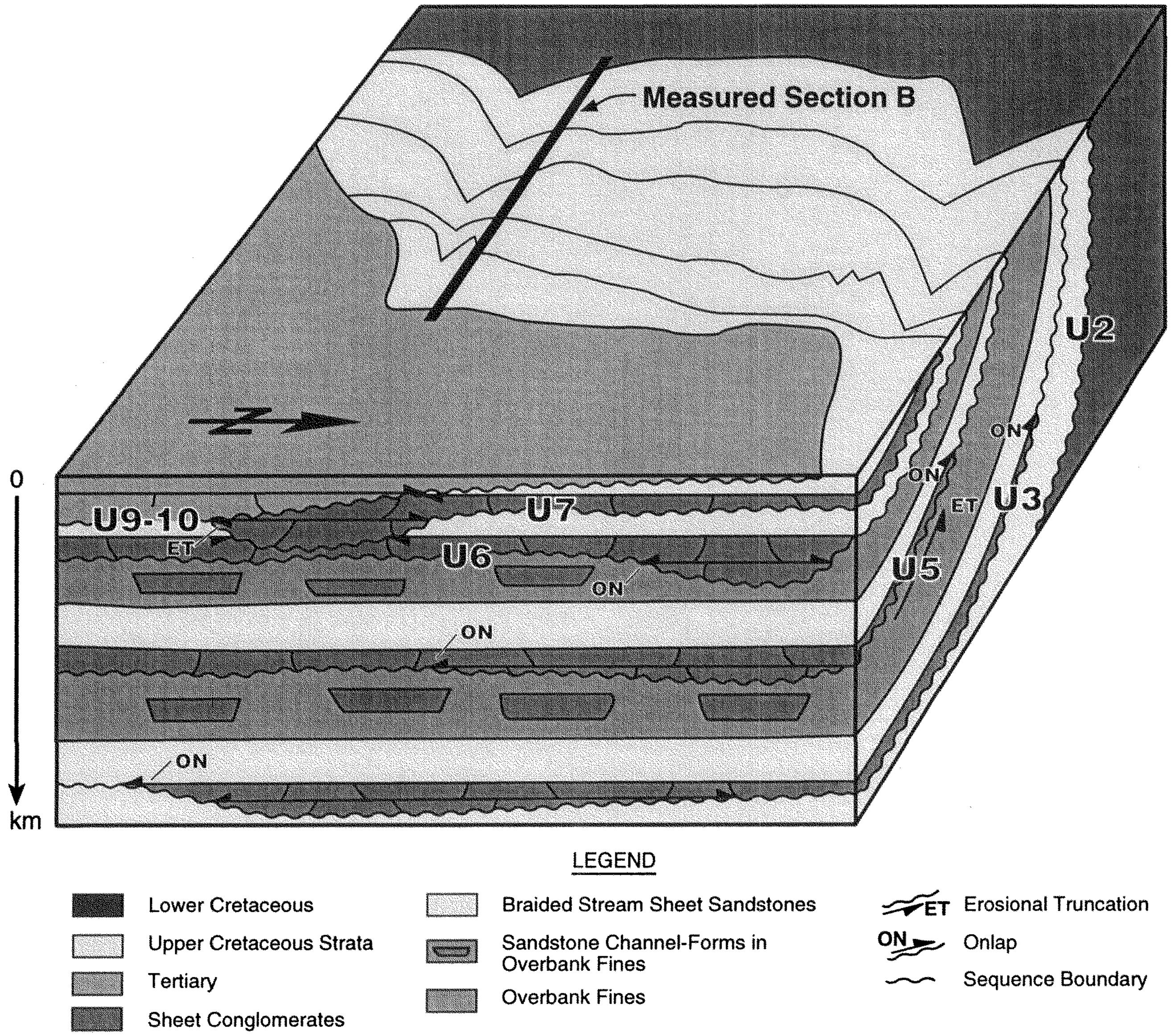

Figure 18. Block diagram and reconstruction of the three-dimensional, depositional sequence architecture in the proximal zone at measured section B (Fig. 12). The block diagram is based on combining facies association identified in the outcrop with geometries observed in aerial photographs.

tion (Fig. 1). North Horn architecture comprises laterally isolated channel forms and occasional lacustrine limestones set in thick red flood plain mudstones.

67.0 Optional Stop 1.3—Angular Unconformity between Red Narrows Conglomerate and Albian through Turonian Cretaceous Strata, Lake Fork

To get there retrace U.S. Hwy. 6 for 1.5 miles toward the west. Turn south onto State Route 89 and cross rail road tracks; take first dust road on left at end of concrete barrier. Proceed east on dust road parallel to Hwy. 6 on south side of valley. Take first fork into small side valley to the right; follow road for about 500 yards into valley. Figure 16 shows a portion of the outcrops located on the east side of the side valley. Horizontal Red Narrows Conglomerate unconformably overlies steeply dipping Cretaceous strata. Fluvial-dominated shoreline deposits beneath U3 are unconformably overlain by quartzite conglomerates and paleovalley fill. A parasequences

Table 2: Lithofacies and depositional environments in the distal zone

Environment	Lithofacies & Bedding Type
Fluvial-dominated Shoreline Deposits	*Tabular sandstones* • low-amplitude crossbeds and trough cross beds with reactivation surfaces, internal scours lined with ripped up shale clasts, shell debris, and log impressions *Mudstones with thin beds of siltstones and muddy sandstones* • wave ripples, wave-form and current flaser ripples, soft-sediment deformation, lags of mollusks, burrows of *Planolites, Palaeophycus,* and *Skolithos* *Lenticular sandstones, shelly banks, and mudstones* • low-angle inclined cross strata, trough cross beds, horizontal planar normal-graded beds, current ripples, wave-form flaser and lenticular ripples, shelly beds, burrows of *Planolites, Palaeophycus, Thalassinoides,* and *Ophiomorpha*
Wave-dominated Shoreline Deposits	*Rippled mudstones and siltstones* • wave-form flaser ripples, wave ripples, small hummocky cross *Hummocky cross-stratified sandstones* • hummocky cross strata, wave ripples, shelly lags, few burrows of *Ophiomorpha* *Trough cross-bedded sandstones* • large-scale, low-amplitude trough cross beds, burrows of *Planolites, Palaeophycus, Thalassinoides, Ophiomorpha,* and *Skolithos* *Scour-based, pebbly sandstones* • trough cross beds
Open-Marine Fine-grained Deposits	*Mudstones with thin beds of wave-rippled sandstones and flaser bedded siltstones to very fine sandstones.* • massive, horizontal-planar bedded, carbonaceous *Micritic limestones*

set of wave-dominated shoreline deposits sharply overlies the valley fill along a flooding surface.

68.0 Return to U.S. Hwy. 6 and proceed east through Red Narrows toward Price.

75.0 Approximate contact between the red flood plain and fluvial deposits of the North Horn Formation and the variegated lake plain mudstones of the Eocene Flagstaff Formation.

76.0 Approximate contact between Flagstaff Formation and the lake-margin to lacustrine limestones and gray to green mudstones of the Green River Formation. Time correlative red-colored, lake plain mudstones with well-defined fluvial channel-forms and small deltas are considered part of the Colton Formation of Early Eocene age.

94.0 Soldiers Summit

106.0 Price River Recreation Area. Paleocene North Horn unconformably overlies Price River Formation of latest Companian and Maastrichtian age along unconformity U8 (Fig. 1).

108.0 **Stop 1.4—Contact between Price River Formation and Castlegate Sandstone**

The Price River Formation outcrops north of the road and comprises *pebbly, channel-form sandstones* and *overbank mudstones and siltstones* deposited in a mixed to suspended-load dominated braided stream and flood plain. In contrast, the underlying, cliff-forming Castlegate Sandstone (*see* cliffs down road toward east) consists of *scour-based, cobble-pebble conglomerates, pebbly sandstones, and sandstones* transported and deposited in laterally coalesced barforms in a bedload-dominated braided stream systems and channel complex. This contrast in depositional architecture is interpreted to reflect a significant acceleration in sediment accommoda-

Figure 19. Photo of tabular sandstones *onlapping (ON) unconformity U3. Sandstones are part of the Upper Turonian Lower Funk Valley Sandstone and strike north-south (left-right). U3 erosionally truncates (ET) underlying open-marine mudstones of the lower to mid Turonian Allen Valley Shale, which rests with sharp contact and flooding surface (FS) of wave-dominated shoreline sandstones of the Sanpete Formation (in lower right).*

tion and subsidence patterns within the foreland basin, probably due to foreland basin segmentation during the Late Campanian.

111.0 **Highway 6 Road Cut, just west of Power Plant, Castlegate Sandstone-Blackhawk Fm. Contact, Helper**
The tall sandstone cliffs on both sides of the road are the Castlegate Sandstone. The coal-bearing strata beneath the sandstone cliffs are the shoreline and coastal plain deposits are part of the Blackhawk Formation of mid-late Campanian age. The Castlegate Sandstone unconformably overlies the Blackhawk Formation along unconformities U7-U8 (Fig. 1).

112.0 **Stop 1.5—Wave-Dominated Shoreline Facies in Gentile Wash Canyon, Blackhawk Fm., Helper**
Turn right into second side canyon; the turn-off is across from a large, gravel strewn pull-out area located on the east side of the road, just down from the Power Plant. The Blackhawk Formation represents a series of stacked, prograding shoreline parasequences or parasequence sets. Individual parasequence sets overlie each other along high-frequency unconformities. Pioneering studies on the regional stratigraphy and depositional settings are by Young (1952, 1955). More recent studies on the parasequence expression and high-frequency parasequence set stacking patterns include, among others, those of Kamola and Van Wagoner (1995), O'Byrne and Flint (1995), and Taylor and Lovell (1995). Six sandstone and coal-bearing members are recognized in the Blackhawk Formation; these are in ascending stratigraphic order, from oldest to youngest, the Spring Canyon Member, Aberdeen Member, Kenilworth Member, Sunnyside Member, and Desert Member. The Spring Canyon and Aberdeen members are exposed in Gentile Wash, while overlying members are truncated by the composite U7-U8 unconformity at the base of the Castlegate Sandstone. The lower Spring Canyon Member in Gentile Wash comprises 4 or possibly 5 parasequences; these are stacked to form a progradational parasequence set. The overlying Aberdeen Member consists of 4 parasequences stacked into a progradational parasequence set. Component depositional facies include *rippled mudstones and siltstones, hummocky cross-statified sandstones, and trough cross-bedded sandstones* deposited in the open-marine and distal lower to lower shoreface environments. Upper shoreface and foreshore sandstones overlain by coastal plain fines and coals comprise the Aberdeen Member.

113.0 **Stop 1.6—Stacking Patterns Summary at the Power Plant, Blackhawk Fm., Helper**
Review of parasequence concepts, summarize the day, and proceed on Route 6 to Price. The top of the Aberdeen Sandstone and progradational parasequence set is exposed in the road cut of Route 6 above the Power Plant. The outcrop is an excellent example of the rapid lateral facies changes that are predicted by the parasequence sedimentology and stacking patterns examined in Gentile Wash.

124.0 Price City Limits

Day 2

Key Topics: Fluvial-dominated shoreline facies (Ferron Sandstone.); parasequence expression, stacking patterns and unconformity types in the distal zone; Upper and Lower Ferron Sandstone; systems tract architecture and sequence expression in the Indianola Group and proximal zone (Sanpete Fm., Allen Valley Shale, Funk Valley Fm., Six Mile Canyon Fm.).

0.0 Leave hotel and proceed south on Route 6
1.0 Exit right onto Hwy. 10 South.
10.0 Emery County Line. The highway runs along the eastern edge of the Wasatch Plateau and descends down-stratigraphic section through the distal deltaic siltstones and parasequences that are equivalent to the Star Point Sandstone (Fig.1). The strata exposed in the slopes of the Wasatch Plateau to the west are, listed in from top to base, the Castlegate Sand-

Figure 20. Photo of the lowstand delta complex of the Coniacian Upper Ferron Sandstone at I-70 (Stop 2.3 in Fig. 2). Deposits of the inner and outer stream-mouth bar above U4 downlap onto pro delta and open-marine mudtsones low U4. The dashed line indicates the approximate position of the correlative conformity (CC) of U3, based on correlations shown in Figure 22. View is to the north. FS–Flooding surface, here parasequence set boundary.

Figure 21. Photo of the same lowstand delta complex. View is to the east into the basin. The coastal plain fines of the lowstand systems tract are abruptly overlain by the open-marine mudstones of the Bluegate Shale.

stone, the Blackhawk Formation, the Masuk tongue of the Mancos Shale, the Emery Sandstone, and the Bluegate tongue of the Mancos Shale.

30.0 Castle Dale, Utah

41.1 Ferron, Utah

47.0 Road to Moore, Utah, on left

52.2 Another road to Moore, Utah, on left

55.4 Turn left onto paved road just after the sign for the town of Emery, Utah; bear left at fork and stay on paved road

60.0 **Stop 2.1—Fluvial-Dominated Shoreline Deposits in Upper Ferron Sandstone, Jim Miller Canyon**

The sandstone cliffs exposed in the canyon are part of the Coniacian-age Ferron delta complex. Mudstones with thin, ripple-laminated and horizontally laminated siltstones, sharp-based, and very fine sandstones with normal-graded, horizontal laminations and current ripples form the base of the outcrop and represent deposition in the pro delta, distal delta front, and proximal delta front. Overlying thickly bedded to massive sandstones with intercutting scours and trough cross beds were deposited in the stream mouth bar. Together these form the *lenticular sandstone, shelly bank, and mudstone* facies association and stack to form a progradational parasequence set or lowstand systems tract.

61.0 **Stop 2.2—Transgressive Systems Tract of the Upper Ferron Sandstone and Bluegate Shale, Jim Miller Canyon**

Turn around and proceed west out of the canyon. As the road leaves the canyon, strata exposed on either side include a range of coastal plain sub environments and lithologies, such as flood plain mudstones, coals, crevasse-splay sandstones and siltstones, and channel-form sandstones. These are in turn abruptly overlain by *open-marine mudstones* of the Bluegate Shale; a few thin tidal parasequences and sandstones are exposed on the north side of the road. As the road traverses the crest and descends the west-dipping backslope of the Ferron hogback, two or possibly three shoreline parasequences are visible in the distance to the west where they form shallow north-south oriented ridges. Together with the tidal parasequences above the Ferron coastal plain, these form the transgressive systems tract to the Ferron lowstand delta complex.

64.6 Return to the main road at the town of Emery, Utah. Turn left onto Hwy. 10 and proceed south.

74.0 Fremont Junction and intersection of Hwy. 10 with I-70. Turn left and get onto I-70 east.

76.5 **Stop 2.3—Lowstand Delta and Incised Valley Fill, Upper Ferron Sandstone, I-70 Road Cut**

Exposures of the Ferron delta complex and coastal plain are found north and south of the Interstate 70 road cut (Figs. 20, 21). *Wave-rippled mudstones, siltstones, and sandstones* at the base are part of the Turonian Tununk Shale. These are abruptly overlain *hummocky cross-stratified* and bioturbated sandstones, which in turn are overlain by delta-front clinoforms. Figure 22 shows U4 at the base of

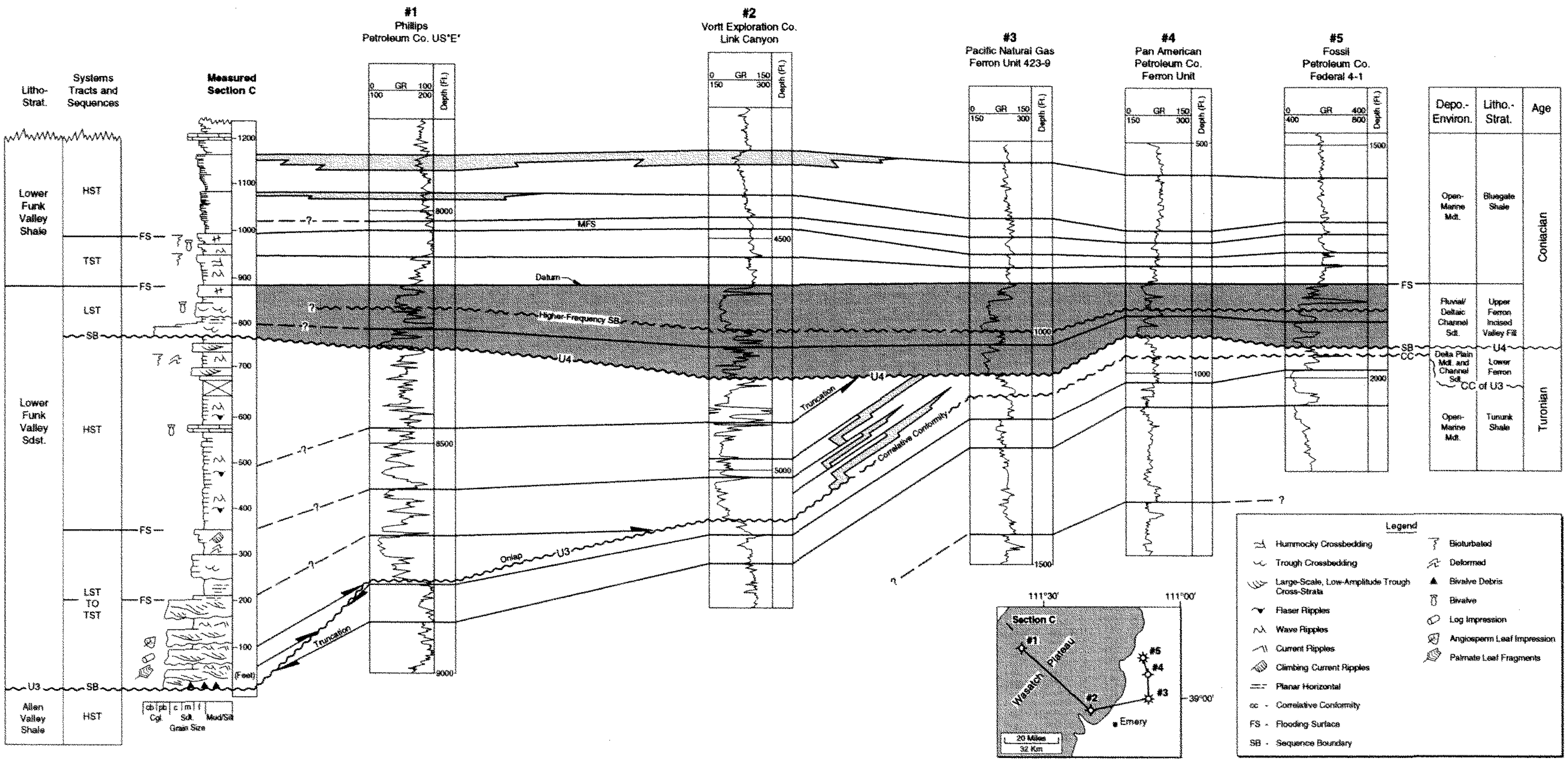

Figure 22. Outcrop and well-log cross section illustrating the sequence-stratigraphic relationship between the Lower Funk Valley Sandstone exposed in measured section C (Figs. 1, 4, 15) and the Upper Ferron Sandstone penetrated in wells located near Stops 2.1 through 2.3 in Figure 2. The interval highlighted in dark grey above U4 is the lowstand systems tract of the U4-U5 sequence in Figure 1. The light-grey shaded units between lines are shoreline sandstones interpreted from logs. MFS–Maximum flooding surface.

the Ferron Sandstone in well #3. The delta-front clinoforms are truncated along their tops by channels of the inner stream-mouth bar, suggesting a high-frequency unconformity; the latter surface is marked also in the well-log cross section. The surface U4 is also exposed in outcrops located on the west side of the plateau.

76.5 Turn around and return to Fremont Junction; proceed west on I-7 toward Salina, Utah.

81.0 Entering the Wasatch Plateau and Fishlake National Forest. Exposures on either side of the interstate are, in order of older to younger, the deltaic and wave-dominated shoreline sandstones of the Emery Sandstone (Late Coniacian through Santonian), the coal-bearing Blackhawk Formation (Campanian), and the Castlegate Sandstone forming the cliffs within the plateau.

91.0 Joe's Graben. Varied-colored mudstones and channel sandstones of the Colton Formation have been faulted down along a series of normal faults. Castlegate Sandstone forms the cliff on along the western edge of the graben.

108.0 Approximate contact between the horizontal red mudstones and siltstones of the Eocene Flagstaff and east-dipping Cretaceous strata. The contact is a composite and angular unconformity consisting of surfaces U5 through U11. The east-dipping Cretaceous strata beneath the angular unconformity are Turonian in age and part to the Lower Ferron Sandstone in Figure 1.

110.0 Exit I-70 and proceed north on Route 28 to the town of Gunnison. Overturned to steeply east-dipping sections of the Jurassic Arapien Shale are exposed to the right (east) of the road in the foothills of the Wasatch Plateau. The valley and the Jurassic strata along the edges form the core to the completely eroded, Tertiary-age Sevier Valley anticline. Cretaceous strata are exposed in respective limbs of the anticline along the edges of the valley and dip to the east and west. They are in turn onlapped by Maastrichtian to Paleocene units similar in facies to the Red Narrows Conglomerate examined in Stops 1.2 and 1.3.

127.0 Gunnison, Utah. Turn right onto U.S. 89 at the north end of town toward Manti, Utah.

133.0 Road cuts through two small hogbacks or blocks of Green River strata, turns northward, and crosses the San Pitch River. The blocks are autochthenous and detached from the underlying Jurassic Arapien Shale via reverse thrusts; movement was down to the west, due to gravity sliding down the west-dipping limb of the Wasatch Monocline. The varied-colored mudstones in the valley and along the base of the Wasatch Plateau on the right are Jurassic Arapien Shale.

Figure 23. Photo of open-marine mudstones of the transgressive and highstand systems tracts of the U4-U5 sequence in measured section C (Fig. 15) at Palisade Lake. The shales are the Lower Funk Valley Shale and form the highstand systems tract (Stop 2.6 in Fig. 2), which overlies the transgressive systems tract (Stop 2.5 in Fig. 2) or top of the Lower Funk Valley Sandstone along the flooding surface FS on the right. Wave-dominated shoreline strata on the left are the base of the Upper Funk Valley Sandstone. View is to the south; strata are vertical and strike north-south. Up-section is to the left (east).

136.0 Gunnison Reservoir on right

137.0 Sterling, Utah. Turn right at northern end of town and proceed on Six Mile Canyon Road toward the plateau and Palisade Lake State Park.

137.5 **Stop 2.4—Systems Tracts, Sequences, and Facies in the Proximal Zone, Indianola Group at Palisade Lake Reservoir**

Pull-over on left side of road at second dust road. Two ridges separated by a valley are visible 500 yards north of the paved road. The lower ridge on the left is the Sanpete Formation and the basal unit of the Indianola Group of Spieker (1946, 1949); strata are vertical and strike north-south in the ridge. The braided stream and wave-dominated shoreline sandstones of the Sanpete Formation are sharply overlain along a flooding surface by open-marine mudstones of the Allen Valley Shale. The Sanpete Formation and the Allen Valley Shale form the U2-U3 sequence (Figs. 1, 15). The ridge to the right is the Lower Ferron Sandstone of Schwans (1988b), which unconformably overlies the shale along U3 (Fig. 19). The associated hiatus spans the Late Turonian (Fig. 1). The section in Figure 15 was measured across the ridges and valley toward

Figure 24. Photo of braided-stream conglomerates of the Six Mile Canyon Formation (Fig. 1) and the U6-U7 lowstand systems tract unconformably overlying the open-marine mudstones of the Upper Funk Valley Shale and U5-U6 highstand systems tract along U6. the outcrop is part of measured section C (Fig. 15); Tertiary strata above U8-11 (upper left) are flat lying and drape over the east-dipping Cretaceous strata. View is to the east. FS–Flooding surface; ON–Onlap.

the plateau. Proceed on road and enter Palisade Lake State Park.

138.5 Stop 2.5—Lowstand-Transgressive Systems Tract of the U4-U5 Sequence, Lower Funk Valley Sandstone and Shale, Palisade Lake Reservoir, Sterling

The strata exposed at the west side of Palisade Lake and the golf course are part of the Upper Funk Valley Sandstone of Schwans (1988b) (Fig. 1) and correlative to the Ferron outcrops seen in previous Stops 2.1, 2.2, and 2.3. Lithofacies include *mudstones with thin beds of wave- and flaser-rippled siltstones and muddy sandstones* overlain by pebbly to coarse grained, *tabular sandstones* with trough cross bedding and low-angle cross bedding; scours overlain by pebble stringers can be found. The sandstones and mudstones are interpreted as braid-delta deposits, possibly deposited within an estuary, and form a progradational parasequence set or lowstand systems tract of the U4-U5 sequence (Figs. 15, 23). They are overlain by a retrogradational stack of wave-dominated parasequences. The valley and golf course at Palisade Lake lie within the open-marine shales of the Lower Funk Valley Shale of Coniacian age (Fig. 1) and are abruptly overlain along unconformity U5 by sandstones of the Upper Funk Valley Sandstone exposed east of the golf course (Fig. 23). The basinward shift in facies across U5 is minor.

139.0 Stop 2.6—Highstand Systems Tracts of the U4-U5 Sequence and the U6 Unconformity, Upper Funk Valley Sandstone and Shale and Six Mile Canyon Fm., Six Mile Canyon, Sterling

Leave palisade Lake Park, turn left golf course and park. The Upper Funk Valley Sandstone exposed along the east side of the golf course were deposited along a wave-dominated shoreline. Lithofacies *wave-rippled mudstones, siltstones, and sandstones, hummocky cross-stratified*, bioturbated, *trough crossbedded sandstones*, and few *scour-based, pebbly sandstones*. The sandstones and mudstones are laterally continuous and form parasequences stacked in an aggradational to minor progradational pattern. The strata are late Coniacian through Santonian in age, based on ammonites and pelecypods (Fig. 1).

Leave parking lot and turn left onto first dust road on the left past entrance to state park; proceed up the dust road into grassy valley below rim of Flagstaff Limestone. Figure 15 shows that in the valley the wave-dominated shoreline sandstones of the Upper Funk Valley Formation are sharply overlain by open-marine mudstones of the Upper Funk Valley Shale of Schwans (1988b). Palynomorphs recovered from the same unit in a nearby well indicate a Santonian age (Villien and Kligfield, 1986). The marine mudstones are sharply overlain along unconformity U6 (*see* east side of valley) by the coarse-grained sandstones of the Lower Six Mile Canyon Formation of the Indianola Group. Basal sandstones are of the *tabular sandstone* lithofacies and exhibit large-scale, trough cross bedding, numerous scours, and impressions and casts of rafted logs. The sedimentary structures and the presence of abundant *Inoceramus* debris in the sandstones are interpreted to reflect deposition in a braid delta. The hiatus associated with U6 incorporates the latest Santonian through possibly Early Campanian (Schwans, 1988b).

140.0 Return to U.S. 89 and the town of Sterling.

Day 3

Key Topics: Piggy-back basin fill and composite unconformities (North Horn Fm., Flagstaff Limestone); Lower Cretaceous basin fill (Pigeon Creek Fm.); Upper Cretaceous basin fill in the proximal zone (Indianola Group Undifferentiated); nonmarine systems tract architecture and sequence expression.

0.0 Leave Sterling on U.S. 89 south.

10.0 Gunnison, Utah. Turn right onto Route 28 north. Road cuts across the southern end of the Gunnison

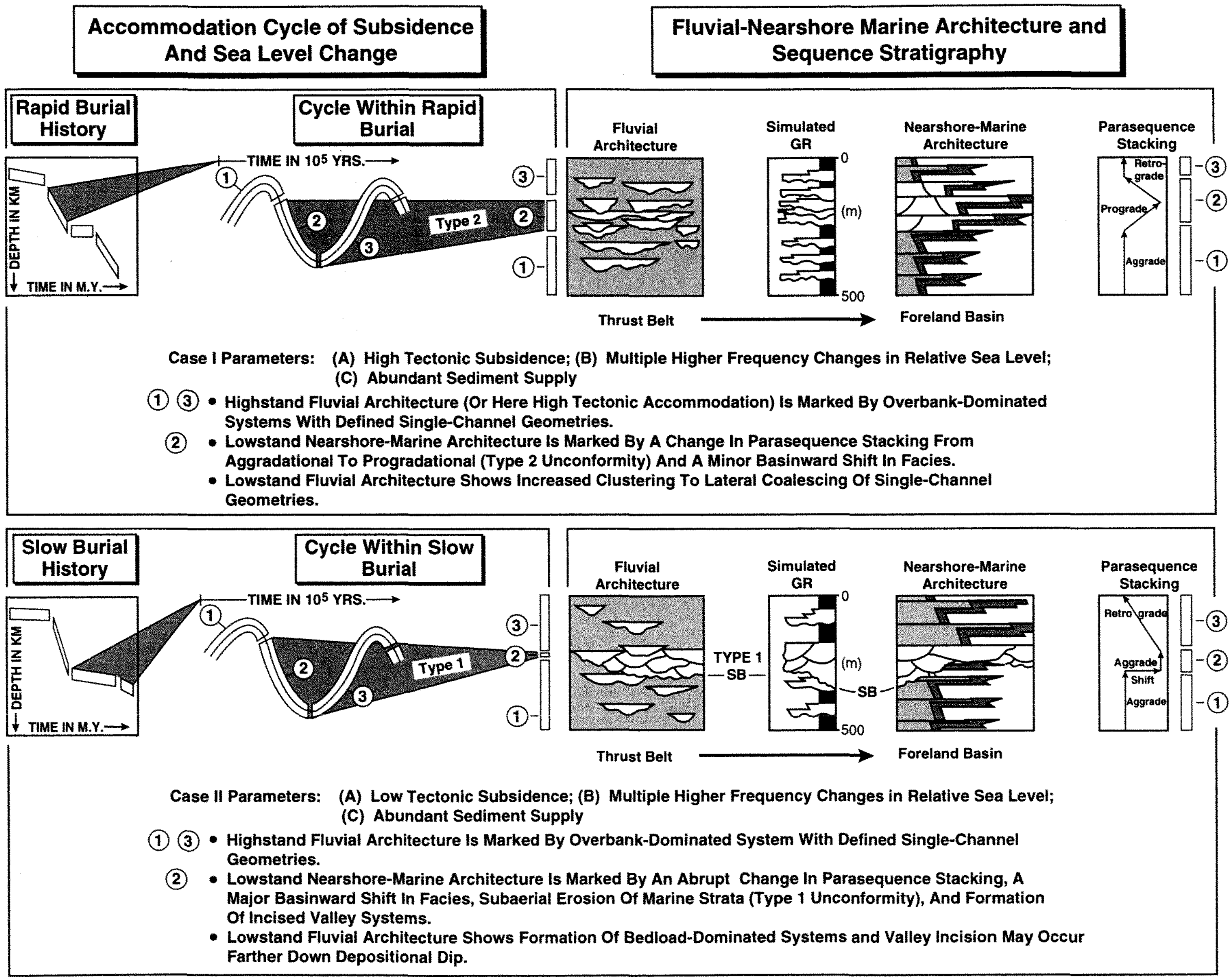

Figure 25. Fluvial and nearshore-marine architecture and parasequence stacking patterns in the accommodation cycle of subsidence and sea level change. The sea level cycle of approximately 10^5 Yr. duration resides on the longer term signal of basin subsidence. Two cases are illustrated.

Plateau; outcrops on the right are lacustrine limestones of the Green River Formation.

17.0 Sevier Bridge Reservoir on left in valley; sign for town of Fayette, Utah. The floor of the valley consists of Jurassic Arapien Shale, which constitute the core of the collapsed Sevier Valley Anticline.

18.0 Turn right behind the town of Fayette onto dust road that leads into Mellor Canyon. The road is marked by a cattle guard and runs straight toward the cliffs.

19.0 **Stop 3.1—Piggy-back Basin Fill and Composite Unconformities, North Horn Fm., Mellor Canyon, Fayette**

The east—dipping conglomerates and sandstones in Mellor Canyon are equivalent to the Campanian Six Mile Canyon Formation examined in Stop 2.6 (Fig. 17). Lithofacies include trough cross-bedded, *scour-based, cobble-pebble conglomerates* grading upward into cross bedded, *pebbly sandstones* and *sandstones*; both represent deposition in gravely and sandy bars on a low-relief alluvial fan. The clastics form the eastern flank of the Sevier Anticline, a thrust-cored uplift of Maastrichtian through Eocene age, and are onlapped along composite surface U8-U9 by folded, *scour-based boulder-cobble-conglomerates*. The latter constitute a paleovalley fill probably age-equivalent to the Red Narrows Conglomerate and record the onset of Sevier Anticline uplift. They are in turn onlapped along U10 by the red *overbank siltstones* and *mudstones* of the North Horn Formation. Conglomerate-filled channels at the base of the North Horn have scoured into the underlying deformed conglomerate unit along U10. The North Horn is onlapped along U11 by the lacustrine mudstones and limestones of the Flagstaff, which eventually overlap the flank of the anticline. For a detailed discussion of piggy back basin formation and the fill see Lawton and Trexler (1991) and Talling et al., (1995).

20.0 Leave Mellor Canyon and return to Route 28; turn right and proceed north.

As the road drops out of the foothills of the Gunnison Plateau a few miles north of Juba Lake, the mountain range visible in the distance to the west (left) is the Canyon Range. The jagged peaks of the range comprise the Precambrian to Cambrian quartzites of the Canyon Range allochthon.

44.0 Levan, Utah. Turn right onto paved road toward Wales and Chester and the Gunnison Plateau.

45.0 Bear right at fork and enter Chicken Creek Canyon. The strata exposed on either side of the canyon are part of the Arapien Shale and include open-marine shales, evaporites, such as gypsum, and thin bedded limestones.

48.0 Uinta National Forest sign

48.5 **Stop 3.2—Facies and Depositional Architecture in the Lower Cretaceous Pigeon Creek Fm. and U1-U2 Sequence, Chicken Creek Campground, Levan**

Turn right into campground located at foot of cliff and park; walk up-canyon on road to where pavement ends. Exposed is the Albian-age upper member of the Pigeon Formation. It forms the cliff and western flank of the Gunnison Plateau (Figs. 6, 7) and consists of stacked and laterally overlapping sheets of horizontally bedded, minor trough cross bedded, pebble-cobble conglomerates with thin, intercalated mudstones. Schwans (1988a) interpreted these as sheetflood fan deposits. Strata of the Barremian to Aptian-age lower member are exposed in the foothills beneath the cliff and consist of stacks of thickbedded, variegated mudstones with intercalated silty-sandy zones, sheets of horizontally-bedded, pebble-sandstones, and sheets of horizontally bedded, chert-pebble and mixed quartzite-carbonate cobble conglomerates. Deposition occurred under a wet-dry, ephemeral climate on gravely sheet-flood fans terminating in a ponded flood plain. The lower member unconformably overlies marginal-marine tidal-flat deposits of the Twist Gulch Formation of Late Jurassic age along unconformity U1.

50.0 **Stop 3.3—Expression of Unconformity U2, Chicken Creek Canyon, Levan**

Return to campground and drive up-canyon past previously visited outcrops. The unconformity U2 separates Lower and Upper Cretaceous strata and is located in the outcrop next to the dust road where reddish colored mudstones and quartzite-carbonate pebble sandstones are overlain by brown to tan-colored, quartzite-pebble to cobble conglomerates. Conglomerates exposed below the surface are of sheet geometry and exhibit mostly horizontal stratification, a red sandstone matrix, few intercalated red mudstones and crossbedded sandstones, and an average maximum clast size of 10 cm. In contrast, conglomerates above U2 overlie well-defined scours, are large-scale lenticular in cross section, and exhibit trough cross bedding, a tan-colored sandstone matrix, and an average maximum clast size of 6 cm. The conglomerate clast composition changes significantly across the surface, indicating a vastly different provenance.

The U2 surface is thus expressed in the measured section (Fig. 12) by (1) al loss in labile clast components, (2) an increase in stable clast types, (3) a significant reduction in maximum clast size, and (4) a change in depositional architecture. Regional correlations show that U2 is onlapped from east to west; the associated hiatus in Chicken Creek Canyon probably spans the latest Albian through Early-Mid? Turonian.

51.5 **Stop 3.4—Facies, Systems Tracts, and Sequence Architecture in the Upper Cretaceous Indianola Group, Upper Chicken Creek Canyon, Levan**
Continue up-canyon and stop at ponds; walk back 100 yards and view outcrops above U6. The measured section in Figure 12 shows five unconformity-bounded and upward fining packages. Lithofacies in the outcrop include *scour-based, cobble-pebble conglomerates* grading upward into cross bedded, *pebbly sandstones* and *sandstones* and reflect traction transport and deposition in gravely and sandy bars in a mixed-load dominated braided stream. The scour-based coarse-clastics are overlain along a sharp surface by *overbank siltstones* and *detrital carbonates* with intercalated trough cross bedded, *pebbly channel-form sandstones*; climbing ripple lamina sets, wedge-planar cross-stratification, trough cross-stratification, contorted bedding, and micro cross-stratified sets, together with an abundance of preserved secondary structures, such as contorted bedding, load and flute casts, rhizoliths, plant impressions, and biogenic traces are ubiquitous. Feeding and foraging traces belong to the *Scoyenia* ichnofacies. Deposition occurred via low-sinuosity, mixed- to suspended-load dominated channels set in a ponded flood plain.

In terms of the foreland accommodation model of Schwans (1995), this change in depositional architecture per sequences reflects the up-dip response of fluvial systems located in the proximal zone to base level changes occurring at the shoreline in the distal zone. In this example, the unconformity U6 is expressed by erosion of underlying strata, a basinward shift in facies across the surface, and onlap against the surface.

53.0 **Stop 3.5—Cretaceous-Tertiary Transition and U8 to U9 Sequence Boundaries in Chris Canyon, uppermost Chicken Creek Canyon, Levan**
Continue on dust road past cliffs with quartzite-boulder conglomerates; these are the paleo-valley fill facies shown in Figure 16. Stop at mouth of Chris Canyon or second dust road branching off to the right. Quartzite-boulder conglomerates identical to those previously encountered in Mellor Canyon (Stop 3.1) and in the Red Narrows (Stop 1.2) occur beneath and above the angular unconformity U9 at the mouth of the canyon. The transition from the Cretaceous to the Tertiary is expressed as a series of angular unconformity, including U8 through U11, that merge on structure toward the emergent anticlines in the Sanpete Valley to the east and the Sevier Valley in the west. In all localities, the conglomerates above U9 show a pronounced angular relationship to those beneath the surface, indicating that erosion and redeposition occurred during uplift and basin subsidence. Pollen recovered from channel coals in Six Mile Canyon (strata above U6 or Stop 2.6) indicate a Late Maastrichtian age for these. The quartzite-boulder conglomerates are onlapped along surface U10 by the red mudstones of the Paleocene North Horn Formation.

59.0 Return to Levan and turn right onto State Route 28 toward Nephi. Turn right onto I-15 North toward Salt Lake City.

ACKNOWLEDGMENTS

We are grateful to M.H. Feeley, Exxon Exploration Company, and A.S. Reeckmann, Exxon Production Research Company, for sponsoring and supporting this field trip. Over the past decades numerous Exxon, Ohio State, and USGS geologists have worked this area. E.M. Spieker and his student from The Ohio State University were true pioneers and visionaries of their time and defined much of the stratigraphy. Their work serves as an inspiration and is the foundation for the sequence stratigraphy presented herein. A.R. Sprague, C. Rossen, and M. Jervey are among many that have worked on the Ferron; their work contributed much to our present understanding of the Ferron. J.C. Van Wagoner defined the sequence stratigraphy of the Blackhawk and the Castlegate. Tom. H. Mooney and Barbara L. Faulkner provided portions of the road log. Last but not least, many thanks to Caroline Peacock for her tireless pursuit of seemingly never-ending logistical problems.

REFERENCES CITED

Allmendinger, R.W., et al., 1986, Phanerozoic tectonics of the Basin and range-Colorado Plateau transition from COCORP data and geologic data. A review, in Barazangi, M., and Brown, L., eds., Reflection seismology. The continental crust: Am Geophys. Union Geodyn Ser. 14, p. 257–267.

Allmendinger, R.W., et al., 1987, Overview of the COCORP 40 degree N transect, western United States: The fabric of an orogenic belt. Geological Society of America Bulletin, v. 98, p. 308–319.

Aubrey, W.M., 1989, Mid-Cretaceous alluvial-plain incision related to eustasy, southeastern Colorado Plateau. Geological Society of America Bulletin, v 101, p 443–449.

Cobban, W.A., 1976, Ammonite record from Mancos Shale of the Castle Valley-Price-Woodside area, east-central Utah· Brigham Young University Geology Studies, v. 22, p. 117–126.

Cotter, E., 1971, Paleoflow characteristics of a Late Cretaceous river in Utah from analysis of sedimentary structures in the Ferron Sandstone. Journal Sedimentary Petrology, v. 41, p. 129–138.

Cotter, E , 1975, Late Cretaceous sedimentation in a low-energy coastal zone. The Ferron Sandstone of Utah, *in* Deltas, Models for Exploration, Broussard, M L S., ed.. Houston Geological Society Publication, p 471–484

DeCelles, P.G., Lawton, T.F., and Mitra, G , 1995, Thrust timing, growth of structural culminations, and synorogenic sedimentation in the type Sevier orogenic belt, western United States. geology, v. 23, p 699–702

Devlin, W.J., Rudolph, K W, Ehmann, K.H., and Shaw, C.A., 1993, The effect of tectonic and eustatic cycles on accommodation and sequence-stratigraphic framework in the Upper Cretaceous foreland basin of southeastern Wyoming, *in* Summerhayes, C.P, Haq, B.U., and Allen, G.P., eds., Stratigraphy and facies associations in a sequence stratigraphic framework· International Association of Sedimentologists Special Publication 18, p 501–520.

Fouch, T.D., et al , 1983, Patterns and timing of synorogenic sedimentation in Upper Cretaceous rocks of central and northeast Utah, *in* Reynolds, M.W., and Dolly, E.D., eds , Mesozoic paleogeography of the west-central United States, Rocky Mountain Paleogeography Symposium 2 Rocky Mountain Sect of S.E.P.M., Denver, CO, p 305–336

Franczyk, K.J., Fouch, T.D., Jonson, R.C., Molenaar, C.M., and Cobban, W.A., 1992, Cretaceous and Tertiary paleogeographic reconstructions for the Uinta-Piceance Basin study area, Colorado and Utah, U S Geological Survey Bulletin 1787, 37 p.

Gardner, M.H , 1993, Sequence stratigraphy of the Ferron sandstone (upper Turonian) of east-central Utah: Ph.D. Dissertation, Department of Geology and Geological Engineering, Colorado School of Mines, Golden Colorado, 405 p.

Gill, J.R., and Hail, W.J , Jr., 1975, Stratigraphic sections across Upper Cretaceous Mancos Shale-Mesa Verde Group boundary, eastern Utah and western Colorado. USGS Oil and Gas Investigations Chart OC-68.

Hale, L A., and Van De Graaf, F.R , 1964, Cretaceous stratigraphy and facies patterns-northeastern Utah and adjacent areas. Intermountain Association of Petroleum Geologists 13th Annual Field Conference, Guidebook to the geology and mineral resources of the Uinta Basin-Utah's hydrocarbon storehouse, p. 115–138

Haq, B.U , Hardenbol, J., and Vail, P.R , 1987, Chronology of fluctuating sea levels since the Triassic: Science, v. 235, p. 1156–1167

Haq, B.U., Hardenbol, J., and Vail, P.R , 1988, Mesozoic and Cenozoic chronostratigraphy and cycles of sea-level change, *in* Wilgus, C.K., Hastings, B.J., Posamentier, H.W, Van Wagoner, J C., and Ross, C.A., and Kendall, C.G. St. C., eds , Sea level change. An integrated approach: Society of Economic Paleontologists and Mineralogists Special Publication 42, p. 71–108.

Heller, P.L., and Paola, C., 1989, The paradox of Lower Cretaceous gravels and the initiation of thrusting in the Sevier orogenic belt, United States Western Interior: GSA Bulletin, v 101, p 864–875.

Jervey, M.T., 1988, *Quantitative geological modeling of siliciclastic rock* sequences and their seismic expression, *in* Wilgus, C.K , et al , eds , Sea-level changes: An integrated approach. Society of Economic Paleontologists and Mineralogists Special Publication 42, p. 47–69

Jordan, T.E., and Flemings, P.B., Large-scale stratigraphic architecture, eustatic variation, and unsteady tectonism. A theoretical evaluation: Journal of Geophysical Research, v,96, p. 6681–6699.

Kauffman, E G , 1977a, Geological and biological overview Western Interior Cretaceous basin. The Mountain Geologist, v 14, p 75–99

Kauffman, E.G , 1977b, Illustrated guide to the biostratigraphically important Cretaceous macro fossils, Western Interior Basin, U S A. The Mountain Geologist, v. 14, p. 225–274

Komola, D L , and Van Wagoner, J C , 1995, Stratigraphy and facies architecture of with examples from the Spring Canyon Member, Blackhawk Formation, Utah, *in* Van Wagoner, J C , and Bertram, G T., eds , Sequence stratigraphy of foreland basin deposits AAPG Memoir 64, p 11–26.

Lawton, T F, 1982, Lithofacies correlations within the Upper Cretaceous Indianola Group, central Utah, *in* Nielson, D L , ed , Overthrust Belt of Utah· Utah Geological Association Publication 10, p. 199–214

Lawton, T.F., 1983, Late Cretaceous fluvial systems and the age of foreland uplifts in central Utah, *in* Lowell, J.D., ed., Rocky Mountain Foreland Basins and Uplifts, Guidebook to Field Conference, Steamboat Springs, Colorado. Rocky Mountain Association of Geologists, Denver, Colorado, p 181–199

Lawton, T.F., 1985, Style and timing of frontal structures, thrust belt, central Utah. American Association of Petroleum Geologists, v. 69, p. 1145–1159.

Lawton, T F, and Trexler, J H , Jr, 1991, Piggy-back basin in the Sevier orogenic belt, Utah· Implications for the development of the thrust wedge: Geology, v. 19, p 827–830

Lawton, T.F, Boyer, S.E., and Schmitt, J.G., 1994, Influence of inherited taper on structural variability and conglomerate distribution, Cordilleran fold and thrust belt, western United states. Geology, v 22, p 339–342

Leithold, E L , 1994, Stratigraphic architecture at the muddy margin of the Cretaceous Western Interior Seaway, southern Utah, Sedimentology, v. 41, p. 521–542.

Martinsen, O J , Martinsen, R.S., and Steidtmann, J.R., 1993, Mesaverde Group (Upper Cretaceous), Southeastern Wyoming. Allostratigraphy versus sequence stratigraphy in a tectonically active area. American Association of Petroleum Geologists, v 77, p 1351–1373

O'Byrne, C.J., and Flint, S., 1995, Sequence, parasequence, and intrasequence architecture of the Grassy Member, Blackhawk Formation, Book Cliffs, Utah, U S A., *in* Van Wagoner, J.C., and Bertram, G.T., eds., Sequence stratigraphy of foreland basin deposits AAPG Memoir 64, p 225–256.

Picha, F, 1986, The influence of pre-existing tectonic trends on geometries of the Sevier orogenic belt and its foreland in Utah, in Peterson, J A , ed , Paleotectonics and sedimentation. A.A.P.G. Memoir 41, p. 309–320

Posamentier, H.W., and Vail, P.R., 1988, Eustatic controls on clastic deposition II—Sequence and systems tract models, *in* Wilgus, C.K., et al., eds , Sea-level changes. An integrated approach. Society of Economic Paleontologists and Mineralogists Special Publication 42, p 125–154

Posamentier, H.W., Jervey, M.T, and Vail, P.R., 1988, Eustatic controls on clastic deposition I—Conceptual framework, *in* Wilgus, C.K., et al., eds , Sea-level changes: An integrated approach. Society of Economic Paleontologists and Mineralogists Special Publication 42, p 110–124

Posamentier, H.W., Allen, G.P., James, D.P., and Tesson, M., 1992, Forced regression in a sequence-stratigraphic framework concepts, examples, and exploration significance. American Association of Petroleum Geologists, v. 76, p. 1687–1709

Royse, F, Jr, (1993), Case of the phantom foredeep. Early Cretaceous in west-central Utah· Geology, v 21, p 133–136

Ryer, T.A., 1981, Deltaic coals of Ferron Sandstone Member of Mancos Shale. Predictive model for Cretaceous coal-bearing strata of Western Interior American Association of Petroleum Geologists, v 65, p 2323–23240.

Ryer, T.A., and McPhillips, M., 1983, Early late Cretaceous paleogeography of east-central Utah, *in* M W, and Dolly, E D , eds , Mesozoic paleogeography of the west-central United States, Rocky Mountain Paleogeography Symp. 2: Rocky Mountain Sect. of S.E.P.M., Denver, CO, p. 253–272.

Schwans, P., 1985a, Fanglomerate deposition in the foreland of the Sevier overthrust belt, control, facies, and timing of earliest syntectonic deposition in Utah, western U.S. [abs.] *in* Proceedings of the 3rd International Fluvial Sedimentology Conference (IFSC), Ft. Collins, Colorado, p. 34.

Schwans, P., 1985b, Depositional controls in the alluvial hinterland of the Cretaceous Interior Seaway: Tectonics, eustasy, and syntectonic sedimentation in central Utah, western U.S.A. [abs.] *in* Programme and Abstracts of Proceedings of International Symposium on Foreland Basins, Fribourg, Switzerland, p. 116.

Schwans, P., 1986a, Late Cretaceous depositional sequence evolution as a result of tectonism, basin subsidence, and sea level change, Turonian to Santonian, west-central Utah [abs.]: American Association of Petroleum Geologists Bulletin, v. 70, p. 1055.

Schwans, P., 1986b, Early Cretaceous depositional sequence evolution in the foreland of the Sevier overthrust belt in west-central Utah [abs.]: Geological Society of America Abstracts with Programs, v. 18, p. 411.

Schwans, P., 1987a, Initial foreland flexure and sedimentation, Early Cretaceous, central Utah [abs.]: Geological Society Abstracts with Programs, v. 19, p. 835.

Schwans, P., 1987b, Sedimentological effects of the tectonic transition from fold-thrust deformation to thrust-cored uplift, proximal Sevier foreland (Six Mile Canyon-Price River-North Horn interval), Campanian-Paleogene of Utah [abs.]: Geological Society of America Abstracts with Programs, v. 19, p. 332.

Schwans, P., 1988a, Depositional response of Pigeon Creek Formation, Utah, to initial fold-thrust deformation in a differentially subsiding foreland basin, *in* Schmidt, C.J., and Perry, W.J., eds., Interaction of the Rocky Mountain Foreland and the Cordilleran Thrust Belt: Geological Society of America Memoir 171, p. 531–556.

Schwans, P., 1988b, Stratal packages at the subsiding foreland basin margin of the Cretaceous foreland basin, Utah, Ph.D. Dissertation, Department of Geology and Mineralogy, The Ohio State University, Columbus, Ohio (Vol. I and II): University Microfilms International, 447 p.

Schwans, P., 1989, Alluvial-marine sequence architecture at a foreland basin margin, Turonian-Santonian, central Utah [abs.], *in* Proceedings to International Conference of Fluvial Sedimentology, Barcelona, Sitges, Spain, p. 215.

Schwans, P., 1990, Sequence stacking and architecture, Cretaceous foreland basin, Utah [abs.]: American Association of Petroleum Geologists Bulletin, v. 74, p. 759.

Schwans, P., 1991, Forcing factors and stratal stacking in the thrust-belt to foreland basin accommodation profile: Late Cretaceous Indianola Group, west-central Utah [abs.]: Geological Society of America Abstracts with Programs, v. 23, p. 95.

Schwans, P., 1995, Controls on sequence stacking and fluvial to shallow-marine architecture in a foreland basin, *in* Van Wagoner, J.C., and Bertram, G.T., eds., Sequence stratigraphy of foreland basin deposits: AAPG Memoir 64, p. 55–102.

Shanley, K.W., and McCabe, P.J., 1991, Predicting facies architecture through sequence stratigraphy—An example from the Kaiparowits Plateau, Utah: Geology, v. 19, p. 742–745.

Spieker, E.M., 1946, Late Mesozoic and Early Cenozoic history of central Utah: U.S. Geological Society Professional Paper 205-D, p. 117–161.

Spieker, E.M., 1949, Sedimentary facies and associated diastrophism in the Upper Cretaceous of central and eastern Utah, *in* Longwell, C.R., ed., Sedimentary facies in geologic history: Geological Society of America Memoir, v. 39, p. 55–81.

Spieker, E.M., and Reeside, J.B., 192, Cretaceous and Tertiary formations of the Wasatch Plateau, Utah: GSA Bulletin, v. 36, p. 435–454.

Standlee, L.A., 1982, Structure and stratigraphy of Jurassic rocks in central Utah: their influence on tectonic development of the Cordilleran foreland thrust belt, in Powers, B., ed., Geologic studies of the Cordilleran thrust belt, volume 1: R.M.A.G., Denver, Colorado, p. 357–382.

Talling, P.J., Lawton, T.F., Burbank, D.W., and Hobbs, R.S., 1995, Evolution of latest Cretaceous-Eocene nonmarine deposystems in the Axhandle piggyback basin of central Utah: Geological Society of America Bulletin, v. 107, p. 297–315.

Taylor, D.R., and Lovell, R.W.W., 1995, High-frequency sequence stratigraphy and paleogeography of the Kenilworth Member, Blackhawk Formation, Book Cliffs, Utah, U.S.A., *in* Van Wagoner, J.C., and Bertram, G.T., eds., Sequence stratigraphy of foreland basin deposits: AAPG Memoir 64, p. 257–276.

Vail, P., Mitchum, R.M., Thompson, S., III, 1977, Global cycles of relative changes of sea level, in Payton, C.E., ed., Seismic stratigraphy-Applications to Hydrocarbon Exploration: A.A.P.G. Memoir 26, p. 83–98.

Vail, P.R., Hardenbol, J., and Todd, R.G., 1984, Jurassic unconformities, chronostratigraphy, and sea-level changes from seismic stratigraphy and biostratigraphy, *in* Schlee, J.S., ed., Interregional unconformities and hydrocarbon accumulations: A.A.P.G. Memoir 36, p. 129–144.

Vail, P.R., and Bowman, S.A., 1987, Sequence stratigraphic concepts applied to stratal patterns in the Cretaceous seaway, western interior of North America [abs.]: Geological Society of America Abstracts with Program, v. 19, p. 875.

Van Wagoner, J.C., 1991a, High-frequency sequence-stratigraphy and facies architecture of the Sego sandstone in the Book Cliffs of western Colorado and eastern Utah, *in* Van Wagoner, Nummedal, D., Jones, C.R., Taylor, D.R., Jennette, D.C., and Riley, G.W., 1991, Sequence stratigraphy applications to shelf sandstone reservoirs: Outcrop to subsurface examples: Field Guide to American Association of Petroleum Geologists Field Conference, September 21–28, 1991.

Van Wagoner, J.C., 1991b, Sequence stratigraphy and facies architecture of the Desert Member of the Blackhawk Formation and the Castlegate Formation in the Book Cliffs of eastern Colorado and western Utah, *in* Van Wagoner, Nummedal, D., Jones, C.R., Taylor, D.R., Jennette, D.C., and Riley, G.W., 1991, Sequence stratigraphy applications to shelf sandstone reservoirs: Outcrop to subsurface examples: Field Guide to American Association of Petroleum Geologists Field Conference, September 21–28, 1991.

Van Wagoner, J.C., Mitchum, R.M., Campion, K.M., and Rahmanian, V.D., 1990, Siliciclastic sequence stratigraphy in well logs, cores, and outcrops: Concepts for high-resolution correlation of time and facies: American Association of Petroleum Geologists Methods in Exploration Series #7, 55 p.

Van Wagoner, J.C., 1995, Sequence stratigraphy and marine to nonmarine facies architecture of foreland basins, *in* Van Wagoner, J.C., and Bertram, G.T., eds., Sequence stratigraphy of foreland basin deposits: AAPG Memoir 64, p. 137–223.

Villien, A., and Kligfield, R.M., 1986, Thrusting and synorogenic sedimentation in central Utah, *in* Peterson, J.A., ed., Paleotectonics and sedimentation: A.A.P.G. Memoir 41, p. 281–307.

Walker, R.G., and Eyles, C.H., 1991, Topography and significance of basin-wide sequence-bounding erosions surfaces in the Cretaceous Cardium Formation, Alberta, Canada: Journal of Sedimentary Petrology, v. 61, p473–496.

Weimer, R.J., 1984, Relations of unconformities, tectonics, and sea-level changes, Cretaceous of Western Interior, U.S.A., *in* Schlee, J.S., ed., Interregional unconformities and hydrocarbon accumulation: A.A.P.G. Memoir 36, p. 7–36.

Yingling, V.L., and Heller, P.L., 1992, Timing and record of foreland sedimentation during the initiation of the Sevier orogenic belt in central Utah: Basin research, v. 4, p. 279–290.

Young, R.G., 1952, Stratigraphic relations in the Upper Cretaceous of the Book Cliffs, Utah-Colorado: Ph.D. Dissertation, Ohio State University, Columbus, Ohio, 147 p.

Young, R.G., 1955, Sedimentary facies and inter tonguing in the Upper Cretaceous of the Book Cliffs, Utah-Colorado, G.S.A. Bulletin, v. 66, p. 177–202.